Scilight

Thermal Science and Applications
https://www.sciltp.com/journals/tsa

Article

Check for updates

Performance Enhancement of an Air Conditioned Classroom Complex with a Dedicated Outdoor Air System

Deen Bandhu * and Maddali Ramgopal

Department of Mechanical Engineering, IIT Kharagpur, Kharagpur 721302, India
* Correspondence: dmishra403@gmail.com

How To Cite: Bandhu, D.; Ramgopal, M. Performance Enhancement of an Air Conditioned Classroom Complex with a Dedicated Outdoor Air System. *Thermal Science and Applications* **2026**, *1*(2), 138–162. https://doi.org/10.53941/tsa.2026.100010

Received: 26 January 2026
Revised: 5 May 2026
Accepted: 7 May 2026
Published: 18 May 2026

Abstract: Providing adequate ventilation for high occupancy buildings is necessary to maintain proper air quality in the conditioned space. However, ventilation increases energy consumption, especially when the outside conditions are hot and humid. Also reheating may be necessary if ventilation leads to increased latent load fraction. The implementation of a suitable energy recovery system can reduce the energy consumption due to ventilation. A dedicated outdoor air unit (DOAU) system comprises an enthalpy wheel, a cooling coil, and a passive desiccant wheel, can be used both for energy recovery as well as reducing reheating requirements. The enthalpy wheel reduces the coil load by pre-cooling the outdoor air, while the passive desiccant wheel eliminates the need for a reheat coil. However, the addition of the DOAU system increases the initial capital investment of the cooling system substantially. Therefore, its use has to be justified through proper performance evaluation. The current study analyses the performance characteristics of a centrally conditioned educational building using a DOAU. To quantify the savings in annual cooling load and energy consumption with DOAU, a detailed analysis of the building is carried out using the well-known Transient System Simulation Tool, TRNSYS. Building simulations are carried out from February to November for hot-humid and hot-dry climates, represented by Kolkata, West Bengal and Jodhpur, Rajasthan, respectively, to assess the suitability of the DOAU system across diverse climatic zones in India. The results show that the required building total load and latent load are maximum in the months of May and July for both Kolkata and Jodhpur. However, Kolkata has a higher building latent load than Jodhpur. Results also indicate 18.0% and 17.5% reductions in annual chiller load and energy consumption for Kolkata, and 6.2% and 5.9% for Jodhpur, with the DOAU system. Implementation of the DOAU system yields better performance during the monsoon compared to the summer months. The overall performance of the DOAU system is better for a hot-humid climate. Therefore, the study is further extended to analyse the performance of the DOAU system under hot-humid conditions. As the performance of the enthalpy wheel deteriorates in terms of sensible and latent effectiveness, the required cooling coil capacity increases. Degradation of latent effectiveness of enthalpy wheel has stronger effect on cooling capacity. The economic analysis is carried out for hot–humid and hot–dry climates. The simple payback period with implementation of the DOAU system, considering constant effectiveness of enthalpy wheel and electric tariff is found to be 4.9 years for Kolkata. The economic analysis shows that the DOAU system is suitable for other climates, such as Jodhpur, only with a higher electricity tariff.

Keywords: ventilation; dedicated outdoor air unit; cooling load, building simulation; annual energy consumption

1. Introduction

The alarming energy demand for buildings to maintain thermal comfort in the coming years is a serious concern for India due to the increased number of indoor occupant hours. Indian buildings account for over 35% of total energy use and have an 8% annual increment rate, expected to increase by 800% in 2047 compared to 2012 [1,2].

With improved living standards and increasing instances of heat waves, air conditioning is becoming essential for every household to maintain healthy indoor air quality and desired thermal comfort. The main drawback of a conventional air conditioning is its high electricity consumption. Almost half of the electricity produced by the developed countries is consumed in building applications, especially in Heating, Ventilation and Air Conditioning (HVAC) [3]. The production of electricity in thermal power plants results in environmental issues (CO_2 emissions), which contribute to climate change.

The main purpose of an air conditioning system is to control temperature, humidity, quality and air motion simultaneously to meet thermal comfort as per ASHRAE standards. Among the four parameters, maintaining the quality of air in the occupied zone is critical and is generally achieved through ventilation. High-occupancy spaces such as classrooms and auditoria require a large amount of ventilation to maintain the quality of air and avoid sick building syndrome (SBS). Effective ventilation strategies in a building can also reduce the risk of airborne spread of dangerous viruses, including COVID-19, and protect the health and well-being of occupants [4].

However, ventilation increases the latent and sensible loads handled by the cooling system substantially, which increases the running cost of the system in terms of higher electricity bills. Studies show that for climatic zones with high temperature and humidity, more than 50% of electricity used by conventional air conditioning is due to cooling and dehumidification of ambient air before it is supplied to the building [5]. For buildings with high ventilation loads, the system must cool the air much below the dew point and then reheat it before supplying it to the occupants' zone. Overcooling the air and then reheating it before supplying it to the occupants' zone increases energy consumption significantly.

The challenges associated with high energy consumption to maintain ventilation standards for high occupant zones in hot-humid climates can be addressed to some extent using a dedicated outdoor air unit (DOAU), which comprises an enthalpy wheel, cooling coil, and desiccant wheel. The basic purpose of the DOAU system is to minimise the chiller cooling load without compromising ventilation standards. An enthalpy wheel with a rotating honeycomb-like structure serves as a heat and mass exchanger that transfers both sensible and latent loads using a coated sorbent material during the interaction between the ventilation and exhaust air streams.

Research shows that among all the available energy recovery systems, the enthalpy wheel offers one of the best solutions for the recovery of heat and moisture between the two air streams. When moist air passes through a desiccant wheel, it results heating and dehumidification while exchanging heat and moisture with conditioned classroom air, which eliminates the need for a separate reheat coil. Desiccant wheels are also very effective in handling latent loads. Thus, a combination of enthalpy and desiccant wheels in a DOAU can significantly reduce ventilation energy consumption.

Furthermore, it is added that the initial costs of the DOAU system are relatively high, and installation requires more space. So, the application of the DOAU system in centrally conditioned buildings like classroom complexes needs to be justified through suitable techno-economic analysis.

The present work investigates an air conditioning system comprising a DOAU and an air handling unit (AHU) for an educational building complex. The system is analyzed to estimate the potential savings in cooling load and energy consumption. Its performance is evaluated under hot-humid conditions in Kolkata and hot-dry conditions in Jodhpur to assess its applicability under different Indian climatic conditions. The results are compared with a conventional air conditioning without a DOAU system.

2. Literature Review and Objectives

Many researchers have conducted studies to investigate and evaluate the performance of energy recovery system-based air conditioning across diverse climates. A chronological overview of studies is presented below:

An early study on the applicability of solid desiccant material in air conditioning was done by Burns et al. [6]. The performance of three hybrid system configurations has been compared with that of a conventional cooling system for a supermarket application with high latent loads. In 1985, Sheridan and Mitchell [7] examined a desiccant based cooling system for hot-dry and hot-humid climatic conditions in Australia. The results of the desiccant cooling system are compared with conventional air conditioning. Jain et al. [8] assessed the applicability of different desiccant based cooling cycles for hot-humid climates. The results demonstrate that the Dunkle cycle offers superior applicability across diverse outdoor conditions relative to ventilation and recirculation cycles. Mumma and Shank [9] compared the DOAU system, consisting of a total energy wheel, cooling-dehumidification

coil and a sensible wheel, with five other approaches, including all-air VAV systems. In this system, conditioned space air is used to reactivate the DOAU system. Based on the results, it can be concluded that the DOAU system offers the best solution among all other configurations for efficiently cooling and dehumidifying outside air without compromising ventilation. Dhar and Singh [10] examine the performance analysis of various hybrid air conditioning systems under different climatic conditions. Finally, it is concluded that a desiccant cooling system performs better and achieves significant energy savings compared with a conventional cooling system in a hot-humid climate. Zhang and Niu [11] estimated energy demand and assessed variations in heating and cooling energy with space temperature and humidity set points for a membrane-based energy recovery ventilation air-conditioning in Hong Kong. Subramanyam et al. [12] developed and investigated the performance of a hygroscopic wheel in an air conditioning for moisture control. Their research indicates that the developed model can supply air at significantly lower dew-point temperatures than conventional systems, at the expense of a slight reduction in COP. Moreover, the system performs better than traditional reheating in achieving equivalent low humidity levels. Zhou et al. [13] used EnergyPlus to simulate and investigate the behaviours of an energy recovery ventilator (ERV) for the building under dynamic conditions. The analysis evaluated the heat recovery ratio relative to energy consumption for the HVAC and ERV at different indoor temperature set points in Beijing and Shanghai. The results indicated that, in summer, the use of ERV becomes less economically viable when the indoor set-point temperature exceeds 24 °C in the Beijing climate. An analysis by Hao et al. [14] shows that integrating chilled ceilings, displacement ventilation, and desiccant-based dehumidification in a hot-humid climate reduces total primary energy consumption by 8.2% compared to conventional systems. This hybrid approach also provides better conditioned air quality and increased occupant thermal comfort. Chen [15] comprehensively reviewed various methods for investigating ventilation performance in buildings and reported that Computational Fluid Dynamics (CFD) models are the most widely used due to their ability to simulate complex airflow, temperature distributions, and contaminant transport, which are difficult to capture with simple analyses. Furthermore, the study emphasises the growing trend of integrating CFD with various simulation tools to improve the prediction accuracy of conditioned buildings while reducing computational costs. Baniyounes et al. [16] investigated the thermal and economic viability of a solar-driven desiccant cooling configuration for a Queensland-based institutional facility. By utilising TRNSYS software to simulate Rockhampton's specific subtropical climate, the researchers analysed the system's capacity for energy conservation, carbon footprint reduction, and overall cost-effectiveness. Guidara et al. [17] proposed a solar-driven solid desiccant model of an air conditioning system intended for commercial buildings in Tunisia. The system performance was evaluated across three operating modes under different climates, i.e., hot-dry, moderate and cold-humid. The findings demonstrate that the system consistently produces supply air capable of maintaining optimal thermal comfort for occupants, regardless of the regional climate. Murray et al. [18] experimentally tested a low-capacity air conditioning with dedicated outdoor air systems comprising a total energy recovery wheel, a cooling and dehumidification coil and a passive dehumidification component, which was reactivated using conditioned space air. The data for analysis of energy performance, i.e., outdoor and return air conditions and chiller water flow rate, are measured during laboratory tests conducted for the Singaporean climate. Jani et al. [19] explored the feasibility of integrating solid desiccant dehumidification with vapour-compression cooling for applications in Roorkee, India. Considering various outdoor conditions, the system's overall performance is evaluated from March to mid-October. The results established that this hybrid approach is highly effective at managing both latent and sensible cooling loads. O'Connor et al. [20] proposed a novel rotary desiccant wheel optimised for passive ventilation by replacing standard honeycomb structures with silica gel-coated radial blades. The system's performance was analysed using CFD and validated through experimental results. The researchers demonstrated that this configuration significantly lowers airflow resistance. The study confirmed that the design effectively manages humidity with minimal pressure drop and operates at reduced regeneration temperatures, offering an energy-efficient solution to enhance space air quality and thermal comfort. Jani et al. [21] adopted a dual approach, combining TRNSYS simulations with experimental validation, to assess the applicability of a hybrid system integrating desiccant dehumidification with standard vapour compression. Their findings suggest that this system could be a feasible alternative to traditional cooling systems for hot-humid climates, achieving better dehumidification of process air while maintaining room thermal comfort. The research conducted by Chen et al. [22] focused on a cooling configuration that utilises a pre-cooling desiccant wheel for high-humidity, high-temperature environments. Their study demonstrated that the efficiency of precooling desiccant wheel air conditioning can be improved by using renewable low-grade heat. Herath et al. [23] focuses to check the suitability of rotary wheels for transferring heat and moisture to the return air of AHUs in centrally conditioned systems in a hot-humid climate. The findings show that the rotary wheel is most recommended for hot-humid zones. Su et al. [24] presented an enhanced dehumidification system that integrates precooling with a recirculated regenerative rotary desiccant wheel. They

verified the feasibility of this system and demonstrated its dehumidification capabilities under various operating conditions, suggesting its potential for practical applications. Bhabhor and Jani [25] conducted a CFD-based investigation of a solid desiccant rotary dehumidifier with different channel geometries for various input parameters. The simulation results across different climate conditions revealed that sinusoidal channels delivered the best performance, yielding superior moisture extraction and supply air thermal properties. The authors also focused on advancing desiccant materials and regeneration processes at lower temperatures to further enhance system performance. Herath et al. [26] conducted a CFD-based study to investigate heat transfer in rotary thermal wheels used in air conditioning for hot-humid zones. The results indicate that wheel performance mainly depends on rotational speed and is optimised between 10–20 rpm. From a geometric point of view, it was recommended that sinusoidal channel geometries with smaller spans and higher heights provide better performance at the expense of higher pressure drop. Tsai and Wu [27] developed and validated a desiccant wheel air conditioning model for all seasons in Taoyuan, Taiwan. The condenser waste heat is used to reactivate the wheel. Their results showed that with an optimised control strategy for the rotary desiccant wheel, about 11.2% savings can be achieved during hot-humid summers. Liu et al. [28] introduced and examined a heat pump-driven outdoor air management device that incorporates both active and passive desiccant wheels. In this configuration, an enthalpy wheel utilises return air to pre-dehumidify incoming outdoor air while simultaneously facilitating regeneration. Analysis revealed that this advanced setup can lower regeneration temperatures by as much as 19.3 °C compared to conventional systems, with the most significant performance gains in a hot-humid climate. Wang et al. [29] carried out a comparative analysis of liquid and solid desiccant cooling systems versus standard split air conditioning units in non-residential buildings for various climatic zones in China. Cho et al. [30] proposed a ventilation solution to address high indoor moisture levels in energy-efficient buildings during cooling seasons. They introduced an energy recovery ventilator system integrated with a cooling coil (ERV-CC) to improve its latent heat recovery efficiency. The ERV-CC system decreased the building load and improved the performance of individual air conditioners. Maqbool and Maddali [31] proposed a hybrid cooling system comprising a low global warming potential (GWP) refrigerant, R-1234yf, a vapour-compression heat pump, and a desiccant wheel. In this system, the ventilation load due to outdoor air is reduced by using an enthalpy wheel. Their results show that the modified hybrid cooling system performs significantly better for low and high building latent loads compared to conventional air conditioning. Bandhu and Ramgopal [32] investigated the performance of a centrally conditioned institutional building equipped with energy recovery wheels regenerated using low-temperature classroom exhaust air. The system's performance is evaluated and compared for different metropolitan cities in India to assess energy and environmental benefits.

The above literature review shows that many researchers have investigated the applicability of energy recovery systems using total energy recovery wheels, sensible wheels, and desiccant wheels to improve the performance of cooling systems. Several researchers have also focused on CFD modelling. These energy recovery systems are well-suited for high-humidity climates. A considerable cooling load and energy saving can be achieved by adding energy recovery wheels to a traditional air conditioning system.

However, the main drawbacks are their high initial cost and requirement for regeneration to ensure continuous operation. The heat source generally used for desiccant wheel regeneration is solar heat or waste heat from other sources. In some small systems, electrical heaters are used for desiccant wheel regeneration. However, the use of low-temperature space air for desiccant wheel regeneration is limited.

It is essential to recognise that the performance of the DOAU system, i.e., the enthalpy and desiccant wheels, may gradually decline over time and ultimately require replacement. Despite their critical role in heat and moisture exchange, there is a significant research gap regarding how the gradual deterioration of energy recovery wheels affects the overall efficiency, cooling capacity, and economic viability of the system over its lifespan.

To address these issues, centrally conditioned educational buildings with and without the DOAU system are modelled using TRNSYS-17. The desiccant wheel and enthalpy wheel integrated with the DOAU are reactivated with conditioned classroom air. The conditioned classrooms with the DOAU system are simulated under different climatic conditions in India, i.e., Kolkata (hot-humid) and Jodhpur (hot-dry), to evaluate its suitability across diverse climatic regions. Using the TRNSYS model, the monthly building and chiller performance, the effect of enthalpy wheel degradation, and the system's economic viability are evaluated. As hourly weather data for Kharagpur (22.33° N, 87.32° E), where the building is located, is not available, the results are obtained for an educational building located in Kolkata (22.57° N, 88.36° E), which is closed to Kharagpur, Bengal, India [33].

3. System Analysis and Methodology

The satellite view of the centrally conditioned educational building (Nalanda complex) situated in IIT Kharagpur, as shown in Figure 1a, is used for the present study. It is divided into Nalanda Rectangular (NR) and

Nalanda Circular (NC) blocks and has a total seating capacity of 12,000 students. The blocks are divided into clusters; each cluster consists of four classrooms. Each cluster has its own DOAU and AHU at roof terrace level, which is connected through duct arrangement.

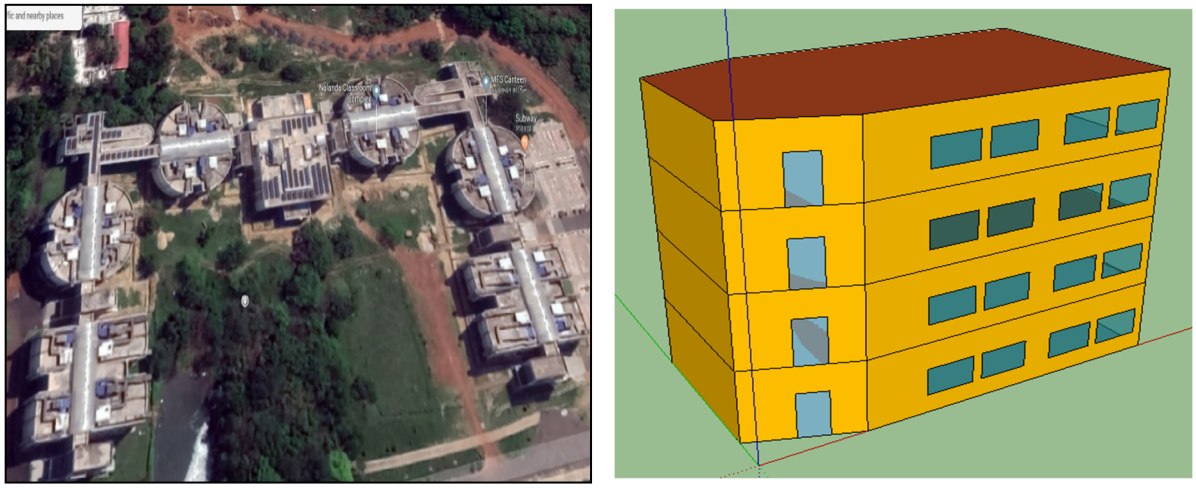

(**a**) (**b**)

Figure 1. (**a**) Satellite image of centrally conditioned educational building complex (**b**) Rectangular classroom cluster considered for this study.

The building material properties required for the calculation of building cooling load, as shown in Table 1, have been taken from ASHRAE Fundamentals-2017.

Table 1. Building construction material properties [34].

Name	Density (kg/m^3)	Thermal Conductivity (W/m-K)	Specific Heat at Constant Pressure, c_p (kJ/kg-K)	Thermal Resistance (m^2-K/W)
Fired Brick	2000	0.9	0.8	-
Cement Plaster	1860	0.72	0.84	-
Concrete	2000	0.6	1	-
Vertical Air Gap	-	-	-	0.3
Horizontal Air Gap	-	-	-	1.5

The floor is made with 250 mm concrete and 10 mm cement plaster. The construction of roof consists of 250 mm concrete, 10 mm cement plaster on both sides, and a false ceiling of 15 mm with 150 mm air gap. The front and side walls (each of area 64.60 m^2) are made of 250 mm fired bricks having 10 mm cement plaster on both sides. The back wall (area 50.80 m^2) which is exposed to outside, contains two layers of normal wall with 10 mm air gap for insulation. The windows are made of 6 mm ordinary glass (Shading Factor, SF = 0.82 & overall heat transfer coefficient, U = 5.7 W/m^2. K). The classroom has a floor area of 261.28 m^2 with a maximum height of 4 m. The north and south walls consist of four windows with an area of 3.75 m^2. Each classroom consists of two doors with an area 3.75 m^2 each, for entry and exit. The total capacity of each rectangular classroom is 240 students. Heat generated from the students is calculated based on the ISO 7730 standard, for seated, very light writing. As per the input provided, the heat generated from lights and electrical equipment inside the classroom is 54.57 kJ/hr per m^2 and 3600 kJ/hr per classroom, respectively.

The geometry of rectangular cluster shown in Figure 1b, is drawn using Google Sketch-up for a Trnsys3d plug-in for type 56 multizone building. The material properties of building are further edited using TRNBuild.

Figures 2 and 3 show the schematic diagram and TRNSYS model of the centrally conditioned educational building complex with a DOAU and AHU. The selected cluster of the NR block has a separate DOAU and AHU for cooling, dehumidifying and filtering the air. The schedule for chiller plant and classroom working hours for weekdays is shown in Table 2. There are no classes scheduled for the weekend.

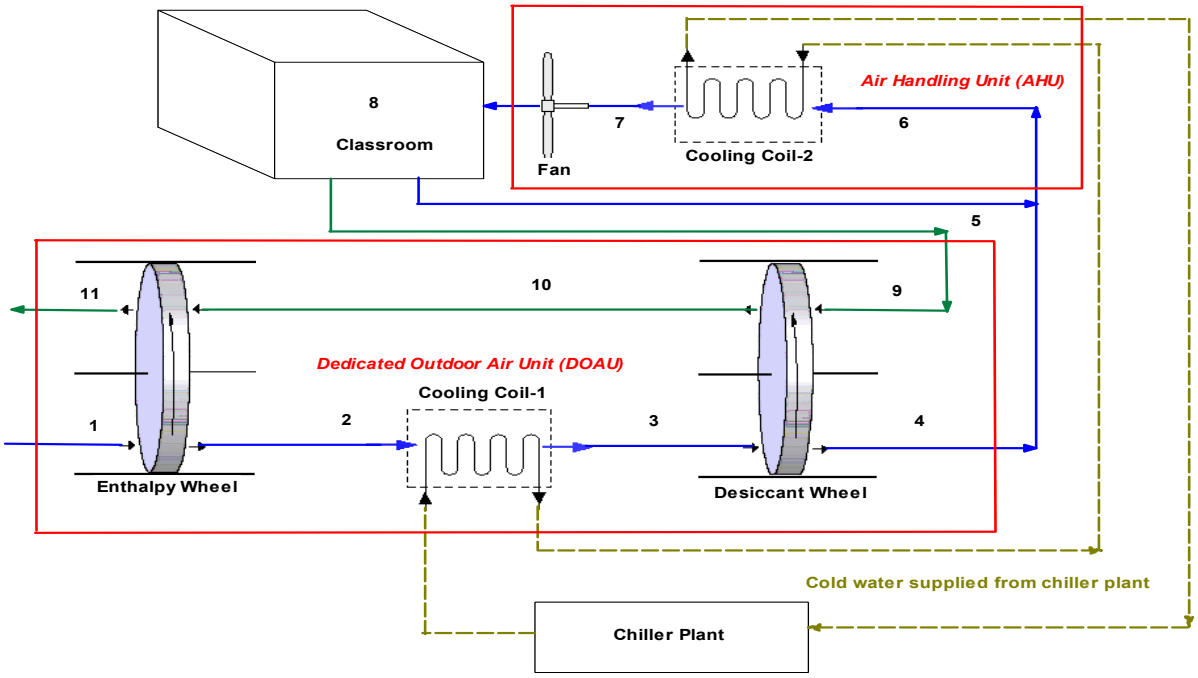

Figure 2. Schematic diagram of the centrally conditioned educational building complex with DOAU and AHU.

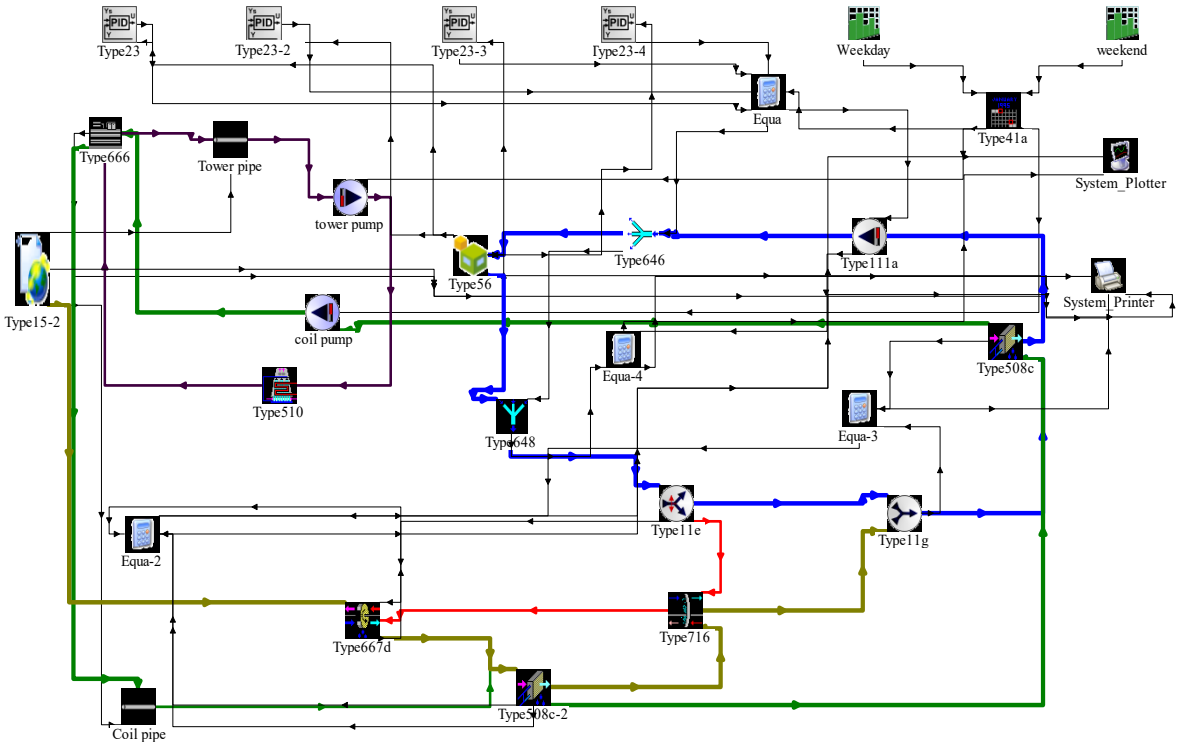

Figure 3. TRNSYS model of the system with DOAU and AHU.

Table 2. Schedule for chiller and classroom working hours from Monday to Friday.

Time	Chiller Schedule	Classroom Schedule
07:00–08:00	ON	OFF
08:00–13:00	ON	ON
13:00–14:00	ON	OFF
14:00–18:00	ON	ON
18:00–07:00	OFF	OFF

TRNSYS-17 is a transient simulation tool used to model thermal systems in Simulation Studio, a graphical user interface that allows system representation using the components library called ‘Types’. Each Type is a set of mathematical equations that process input variables and parameters to generate the outputs.

A detailed description of TRNSYS component types and their applications in the analysis of a conditioned classroom complex with DOAU system is shown in Table 3.

Table 3. List of TRNSYS components used for simulation [35].

Sr. no.	Component Type	Component Name	Description
1	15	Weather data processor	This component is used for analysis of weather data at regular time interval for a particular location from an external file available along with TRNSYS package.
2	65	System plotter	This component is used for online graphical plotter of desired variable during simulation. The variable can be plotted for any time interval during whole year.
3	25	System printer	This component is used for output/ print of any required variable for specific time interval. The file can be further transported into word of excel format for analysis.
4	56	Multi-zone building /Classroom complex	This component is used for model the thermal behaviour of multizone building. The material properties and other parameters of the building are further edited using TRNBuild.
5	667	Enthalpy wheel	This component models a rotary enthalpy wheel for energy recovery in a centrally conditioned classroom complex. The wheel model is based on a constant effectiveness and minimum capacitance approach.
6	716	Desiccant wheel	This component models a rotary desiccant wheel coated with hygroscopic material, i.e., silica gel. The main purpose of this wheel is to avoid the requirement of a heating coil and remove additional moisture associated with the supply air.
7	508	Cooling coil	This component models a cooling coil using a bypass approach. The air, as it passes through the coil, is cooled and dehumidified.
8	Equa	Equation	This tool is used for adding new equation during simulation.
9	666	Water cooled chiller	This component is used for simulation of a water cooled chiller. The chiller works on vapour compression cycle and its performance depends on external text file provided on catalogue data.
10	510	Cooling tower	This component is used to model the closed circuit cooling tower.
11	11	Tee-Piece (splitter/mixer)	This component is used for pipe or duct tee-pieces, mixers, and diverters.
12	111	Variable speed fan	This component is used for modelling a fan. This fan can be operated from zero to its rated speed.
13	646	Air flow diverter	This component model a supply air plenum. It can be used for diversion of one air stream into different as per requirement.
14	648	Air flow mixer	This component model a return air plenum. It can be used for mixing of different air streams.
15	14	Forcing function	This component is used for scheduling. (day or week)
16	41	Load profile sequencer (Weekdays and Weekends)	This component is useful for organizing daily/weekly profiles generated by Type 14.
17	31	Pipe (coil Pipe/tower pipe)	This component models the thermal behaviour of a flowing fluid in a pipe using variable-sized segments.
18	110	Variable speed pump (coil pump/tower pump)	This component is used for model the variable speed pump. The pump used for maintaining any outlet mass flow rate between zeros to rated.
19	23	PID controller	The PID controller is used to calculate the control signal required to maintain the controlled variable at the set point.

Figure 4 represents the psychrometric properties of air at different states with the DOAU and the AHU under a hot-humid climate. The fresh outdoor air at state 1, as shown in Figure 2, is supplied to the enthalpy wheel, where it undergoes cooling and dehumidification (1–2) while transferring heat and moisture to the outgoing exhaust air (10–11). At state 2, the air proceeds to cooling coil-1 for further cooling and dehumidification process (2–3), employing chilled water sourced from the central water cooled chiller plant. At State 3, the air is treated within the passive desiccant wheel, which facilitates additional heating and dehumidification (3–4) by exchanging heat and moisture (9–10) with exhaust air from the conditioned classroom. From the figure, it is observed that the regeneration air entering the desiccant wheel (State 9) has a higher specific humidity than the process air entering the desiccant wheel (State 3). Even under these conditions, the passive desiccant wheel is able to transfer moisture effectively through the wheel matrix, resulting latent cooling effect. This behaviour is due to the hygroscopic nature of the desiccant material, which shows higher moisture sorption capacity at elevated relative humidity (RH). Therefore, moisture transfer in a passive desiccant wheel is driven by the difference in relative humidity rather than the difference in specific humidity [18]. At State 4, the supply air is mixed with a portion of the recirculated air from the classroom shown as state 5, for further cooling and dehumidification (6–7) at cooling coil-2, continuing to exchange heat with the chilled water. Finally, this processed air is supplied to space for achieving desired conditions (DBT = 26 °C, RH = 50%) required for thermal comfort.

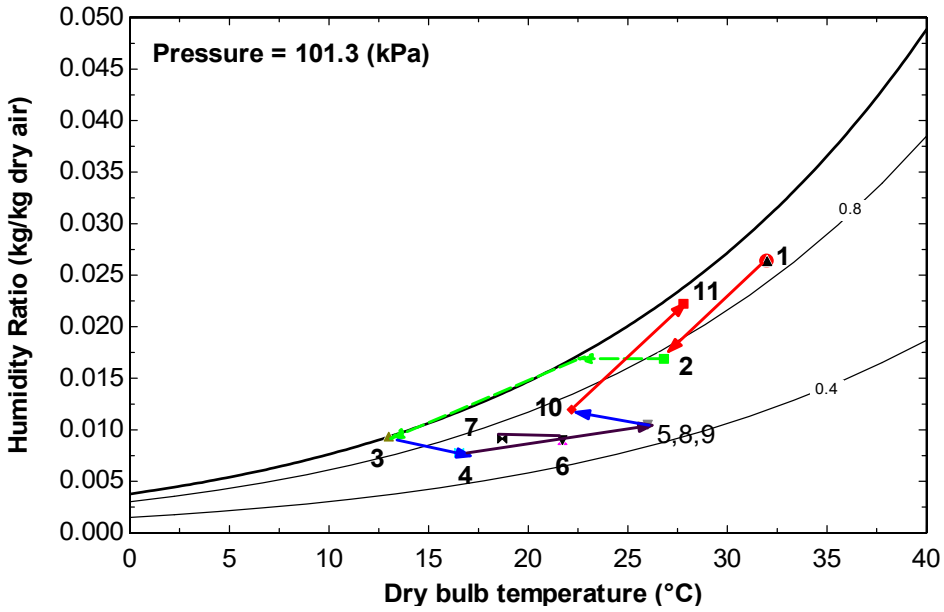

Figure 4. Psychrometric representation of different states of a centrally conditioned educational building with DOAU and AHU.

3.1. Energy Analysis

3.1.1. Cooling Coil

Conventional air conditioning systems normally use a single coil to cool and dehumidify the outdoor air to achieve the desired indoor conditions. However, in the present study, the enthalpy wheel, coil-1, the desiccant wheel, and coil-2 are used to achieve the desired space conditions for thermal comfort of the occupants.

Type 508 from the HVAC component library of TRNSYS simulation studio is selected as cooling coil-1 and 2 for cooling and dehumidification of incoming outdoor air, while exchanging heat and moisture with the chilled water supplied from the water cooled chiller Type 666. The mass flow rate ($\dot{m}$), dry bulb temperature (T_d) and specific humidity (ω) of air at the inlet and exit of cooling coils are connected through an equation component (Equa) for the calculation of both the cooling coil capacities, as shown in Figure 3.

Cooling coil capacities of coil-1 and 2 are calculated as follows:

$$Q_{C,1,S} = \dot{m}_2 \, c_p \left(T_{d,2} - T_{d,3}\right) \tag{1}$$

$$Q_{C,1,L} = \dot{m}_2 \, h_{fg} \left(\omega_2 - \omega_3\right) \tag{2}$$

$$Q_{C,1,t} = Q_{C,1,S} + Q_{C,1,L} \tag{3}$$

$$Q_{C,2,S} = \dot{m}_6 \, c_p \left(T_{d,6} - T_{d,7}\right) \tag{4}$$

$$Q_{C,2,L} = \dot{m}_6 \, h_{fg} \left(\omega_6 - \omega_7\right) \tag{5}$$

$$Q_{C,2,t} = Q_{C,2,S} + Q_{C,2,L} \tag{6}$$

The total cooling capacity of both coils is calculated from Equation (7). The design of the chiller is based on total cooling coil capacity to handle the building and ventilation cooling load requirements.

$$Q_{c,t} = \left(Q_{C,1,t} + Q_{C,2,t}\right) \tag{7}$$

3.1.2. Chiller Performance

Component type 666 in TRNSYS Simulation Studio is used to model a water cooled vapour compression chiller, based on performance maps that account for variations in operating conditions and part load behaviour, making it suitable for simulating a central conditioned classroom complex with DOAU and AHU. The total cooling capacity calculated from Equation (7) by the air side cooling coil (Type 508) referred to as chiller cooling load ($Q_{chiller}$) and is supplied to the chiller as input. It represents the instantaneous cooling demand that the chiller must meet. The available cooling capacity (Q_{avil}) of the chiller at the given chilled water and condenser water temperatures is first determined using the capacity ratio (R_c) and chiller rated capacity (Q_{rated}) from Equation (8) [35,36].

$$R_c = \frac{Q_{avil}}{Q_{rated}} \tag{8}$$

The part load ratio (*PLR*) of the chiller is calculated from Equation (9):

$$PLR = \frac{Q_{chiller}}{Q_{avil}} \tag{9}$$

Q_{met} is defined as the cooling actually delivered by the chiller at a given simulation time step to satisfy the instantaneous cooling demand imposed by the air side system. It is used as the input for calculating the chiller electrical power consumption [37,38].

$$Q_{met} = \begin{cases} Q_{chiller}, & \text{if} \quad PLR \leq 1 \\ Q_{avil}, & \text{if} \quad PLR > 1 \end{cases} \tag{10}$$

Once Q_{met} is known, Type 666 calculates the Fraction of Full Load Power (F_{PL}) as a function of *PLR* shown in Table 4. The chiller power ($P_{chiller}$) is the input power required for the operation of the chiller unit and is calculated using Equation (11).

$$P_{chiller} = Q_{met} \, \frac{F_{PL}}{COP_{rated}} \tag{11}$$

The effective operating coefficient of performance (*COP*) of the chiller under part load conditions is calculated by using Equation (12).

$$COP = \frac{Q_{met}}{P_{chiller}} \tag{12}$$

The above mentioned equations are used for calculation of hourly cooling capacity (kW) and input power (kW) of the chiller with and without the DOAU system. The annual chiller load (GJ) and energy consumption (GJ) are calculated by integrating total hourly loads over the year.

Table 4. Variation of F_{PL} with *PLR* [39].

Part Load Ratio (*PLR*)	Fraction of Full Load Power (F_{PL})
0.0000	0.0000
0.2500	0.2497
0.5000	0.4956
0.7500	0.6902
1.0000	1.0000

The total and percentage savings of chiller cooling load and energy consumption with the DOAU system are calculated using Equations (13) to (16).

$$Q_{chiller,Saving} = Q_{chiller,Conv} - Q_{chiller,DOAS} \tag{13}$$

$$\%\ saving = \left(Q_{chiller,Saving} \,/\, Q_{chiller,Conv}\right) \times 100 \tag{14}$$

$$P_{chiller,Saving} = P_{chiller,Conv} - P_{chiller,DOAS} \tag{15}$$

$$\%\ saving = \left(P_{chiller,Saving} \,/\, P_{chiller,Conv}\right) \times 100 \tag{16}$$

3.2. Economic Analysis

The Implementation of the DOAU system (enthalpy and desiccant wheel) with air conditioning to maintain desired thermal comfort inside classrooms not only increases the system's size but also increases its overall cost. Furthermore, the performance of the enthalpy and desiccant wheels degrades over time, which may necessitate the replacement of the wheels.

For analysis, the life of the enthalpy and desiccant wheel is considered to be 15 years, the life of the chiller and tower pump is 10 years, and the overall life of the chiller plant is 25 years, as specified by the manufacturer [40–43].

A detailed economic analysis is required to determine the feasibility of the DOAU system for a centrally conditioned educational building complex for hot-humid and hot-dry climates. All costs associated with the calculation of Life cycle cost (LCC) with and without DOAU system, as shown in Table 5, are converted from Indian rupees (INR) to US dollars (USD) to maintain consistency, facilitate comparison, and ensure broader applicability of the results. It will also help the reader from different geographical areas to easily understand and interpret the results. All costs are converted from INR to USD using a fixed exchange rate of 1 USD = 89.7 INR (mid-market exchange rate as on 25 December 2025). The cost details of the chiller and DOAU system are obtained from local contractors and manufacturers [40–43]. AHU and ductwork costs are not considered in the present study, as their marginal difference with and without the DOAU system is negligible.

Table 5. Cost associated with and without the DOAU system for LCC calculation.

Component Cost	Cost (USD Thousands) without DOAU (Chiller Capacity: 105 TR)	Cost (USD Thousands) with DOAU (Chiller Capacity: 84 TR)
Chiller machine cost	109.1	86.3
Cooling tower cost	19.1	15.1
Cooling water pump cost	4.4	3.5
Chiller water pump cost	3.8	3.0
DOAU system cost	0.0	29.9
Total installation cost	24.1	26.5
Total initial cost (C_0)	160.5	164.4
Annual energy cost (C_E) (Electricity tariff: USD 0.10/kWh) [44] for Kolkata	7.8	6.4
Annual maintenance and repair cost (C_{MR})	1.9	2.4
Salvage value (S_n) (20% of initial cost) [45]	32.1	32.9

The life-cycle cost (LCC) of a centrally conditioned educational building complex, with and without DOAU, is calculated using Equations (17) and (18) as described below [46–49].

$$LCC_{conv} = C_0 + C_{R,Pump}\left(\left(\frac{1}{(1+d)^{10}}\right) + \left(\frac{1}{(1+d)^{20}}\right)\right) + (C_E + C_{MR})\left(\frac{(1+d)^n - 1}{d\,(1+d)^n}\right) - S_n \tag{17}$$

$$LCC_{DOAU} = C_0 + C_{R,Pump}\left(\left(\frac{1}{(1+d)^{10}}\right) + \left(\frac{1}{(1+d)^{20}}\right)\right) + C_{R,DOAU}\left(\frac{1}{(1+d)^{15}}\right) + (C_E + C_{MR})\left(\frac{(1+d)^n - 1}{d\,(1+d)^n}\right) - S_n \tag{18}$$

The simple payback period (*PBP*) with the DOAU is calculated using Equation (19) as under,

$$PBP = \frac{(C_{0_{DOAU}} - C_{0_{conv}})}{((C_E + C_{MR})_{conv} - (C_E + C_{MR})_{DOAU})} \quad (19)$$

where, LCC_{conv} and LCC_{DOAU} denote the Life cycle cost with conventional air conditioning and life cycle cost with DOAU based air conditioning. C_0 refer total initial cost of the system, C_R shows replacement cost of chiller water pump, cooling water pump and DOAU system (e.g., enthalpy and desiccant wheel), C_E used for annual energy cost, C_{MR} represents annual maintenance and repair cost, S_n denote salvage value cost at the end of life (20% of C_0), 'd' and 'n' denotes discount rate (8%) and lifespan of cooling system (25 years) considered for present study.

4. Results and Discussion

Hourly analysis of ambient DBT (°C) and RH (%) for Kolkata and Jodhpur from February to November, as shown in Figures 5 and 6, reveals that only a few working hours of classrooms during the summer and monsoon months are naturally comfortable [33]. In contrast, employing an air conditioning system for cooling and dehumidification maintains a comfortable environment for almost all working hours in hot-humid climates. Based on these findings, DOAU system-based air conditioning is identified as the most suitable solution for the hot-humid climate of Kolkata.

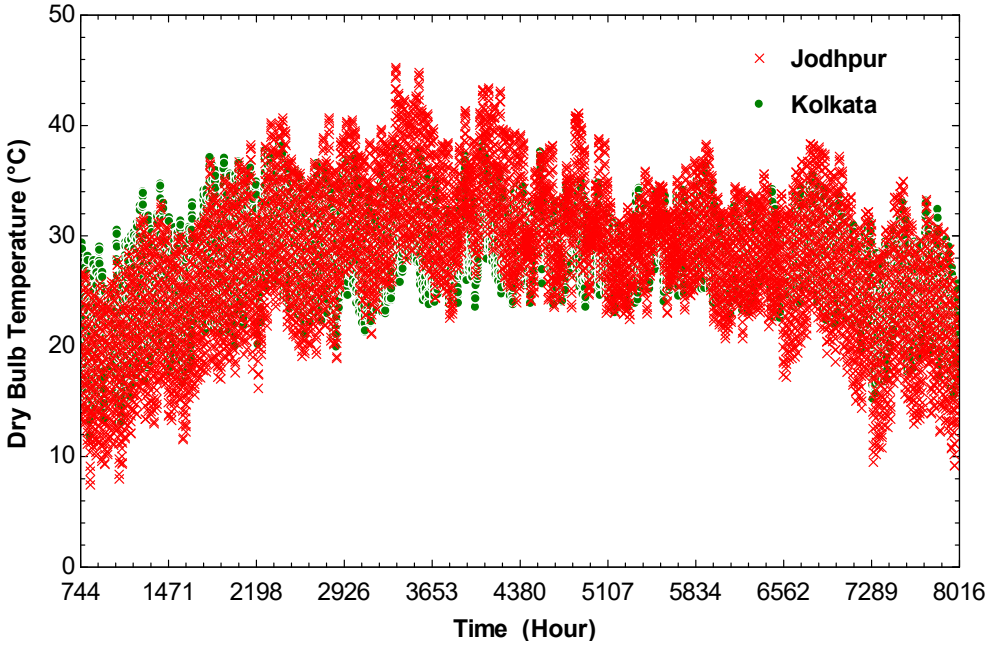

Figure 5. Hourly variation of ambient temperature for Kolkata and Jodhpur.

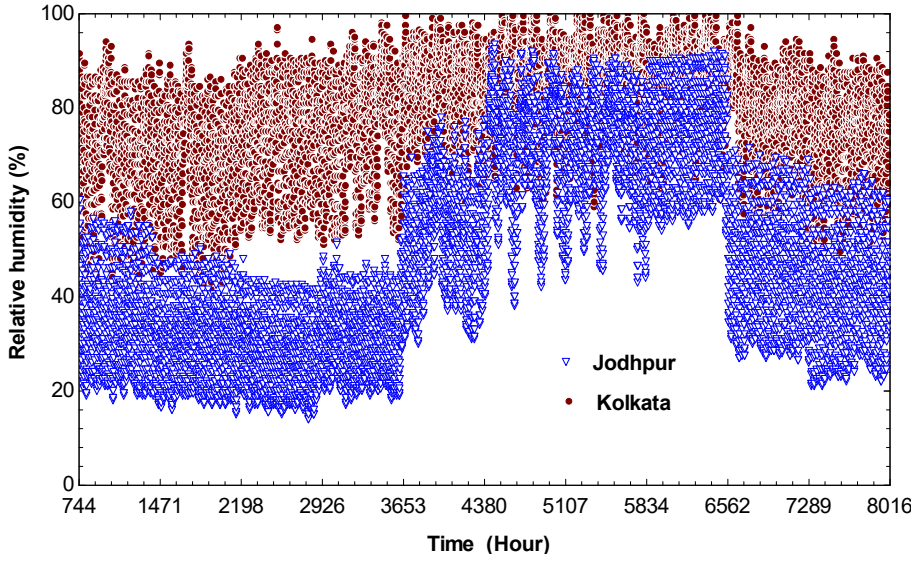

Figure 6. Hourly variation of ambient relative humidity for Kolkata and Jodhpur.

4.1. System Validation

The validation of the developed model of the centrally conditioned educational building complex with the DOAU system is carried out using a combination of previously published literature and manufacturer data available with the building manual for summer and monsoon conditions [41].

The trends of psychrometric properties (DBT and RH) at different states of DOAU-based air conditioning, as shown in Figure 2, operated under similar outdoor and indoor conditions, are summarised in Table 6. The DBT and RH at different states show reasonable agreement between the simulated results, manufacturer data, and a previously published paper, indicating that the simulation model captures the correct physical trends.

Table 6. Validation of the results with Manufacturing data and available literature.

S no	Parameters		Psychrometric Properties at Different States of Conditioned Air with the DOAU System								
			1	**2**	**3**	**4**	**5, 8, 9**	**6**	**7**	**10**	**11**
1.	Manufacture data (Summer)	DBT (°C)	37.8	27.8	10.2	14.2	26.0	23.3	15.8	21.4	35.6
		RH (%)	50.0	63.5	99.6	63.6	45.0	47.0	76.0	67.6	51.2
	Simulation result	DBT (°C)	36.8	27.6	8.2	11.4	26.4	23.4	15.7	23.1	32.2
		RH (%)	51.0	64.8	99.9	68.6	52.4	61.9	93.0	74.9	59.6
2.	Manufacture data (Monsoon)	DBT (°C)	32.2	25.6	10.1	14.2	26.0	23.3	15.7	21.4	30.8
		RH (%)	75.0	78.2	99.6	63.6	45.0	47.0	76.0	67.6	76.4
	Simulation result	DBT (°C)	32.3	25.3	8.0	10.5	26.1	21.2	14.7	21.6	28.7
		RH (%)	74.3	78.4	100	78.1	58.8	70.9	96.7	80.8	80.3
3.	Murray et al. [18]	DBT (°C)	30.0	23.3	13.0	18.0	24.9	-	18.0	19.2	-
		RH (%)	55.3	72.3	93.6	61.4	57.0	-	61.4	87.2	-
	Simulation result	DBT (°C)	32.1	26.1	7.9	11.3	26.3	23.3	15.7	22.9	29.0
		RH (%)	55.5	65.8	99.2	69.1	56.8	60.9	95.0	74.0	61.8

The purpose of this validation is to ensure a preliminary assessment of system performance, rather than an exact prediction. Based on the above comparison results, the developed model can be considered reliable for evaluating the performance of a conditioned educational building with the DOAU system for energy and economic analyses under different climatic conditions.

4.2. System Performance

Figure 7 shows the variation in building total cooling and latent cooling loads for Kolkata and Jodhpur from February to November, based on the classroom schedules presented in Table 2. From the graph, it can be concluded that the total building loads for Kolkata and Jodhpur are almost equal during monsoon months. However, the Kolkata building has a higher latent load due to more humid ambient conditions. The total building load and latent load are highest for May and July, respectively, for both Kolkata and Jodhpur.

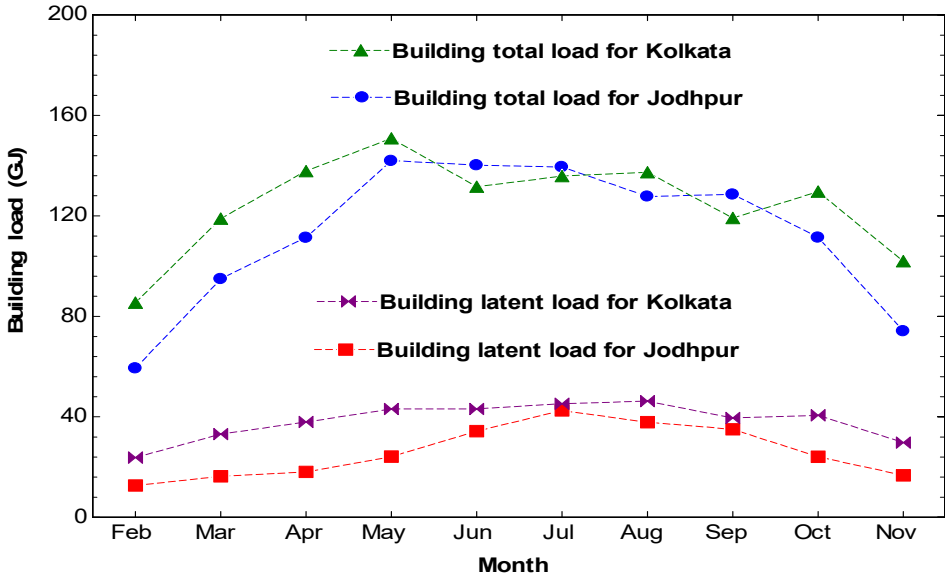

Figure 7. Variation of monthly building cooling loads for Kolkata and Jodhpur.

A detailed performance evaluation of the DOAU system is further carried out for Kolkata to accurately predict system behaviour under hot-humid climatic conditions. Figure 8 shows the variation of monthly peak building total cooling and sensible cooling loads from February to November, as per classroom schedules, for Kolkata. The peak building total cooling load is maximum for May due to high solar radiation, while the latent cooling load is maximum for July when outdoor air is humid.

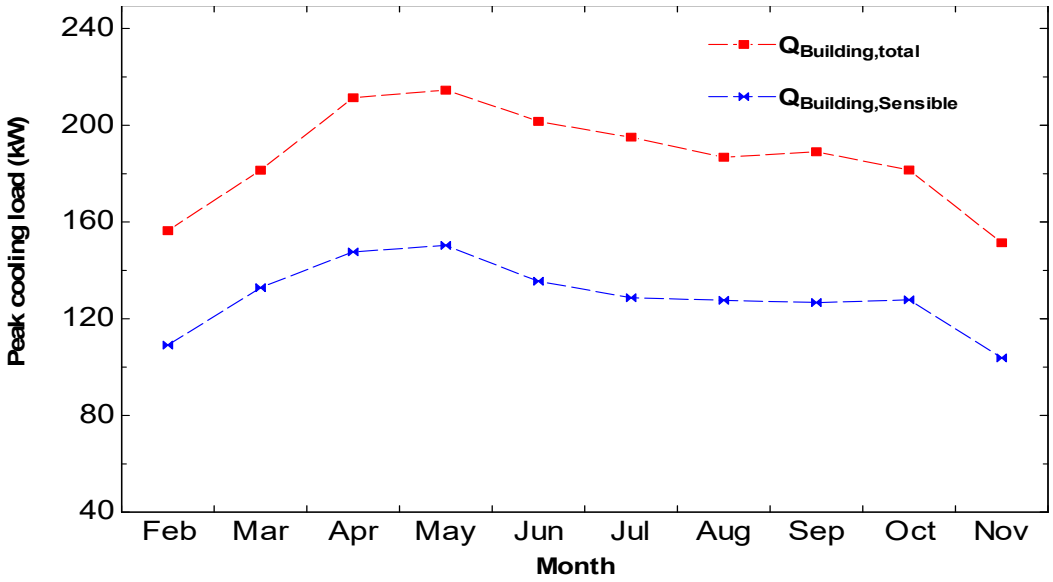

Figure 8. Variation of maximum monthly building cooling loads for Kolkata.

Figure 9 illustrates the monthly variation of the total building cooling load, chiller cooling load and chiller energy consumption, with and without the DOAU system, for the centrally conditioned classroom from February to November, for Kolkata. The DOAU system incorporates an enthalpy wheel with sensible effectiveness of 0.67 and latent effectiveness of 0.71 [50,51], which is used in this analysis. The results indicate that the maximum reduction in chiller cooling load and chiller energy consumption occur during the monsoon months (June–September) with the DOAU system compared to the summer months. This is mainly due to the increased outdoor air humidity during the monsoon season, which improves the latent heat recovery potential of the enthalpy wheel.

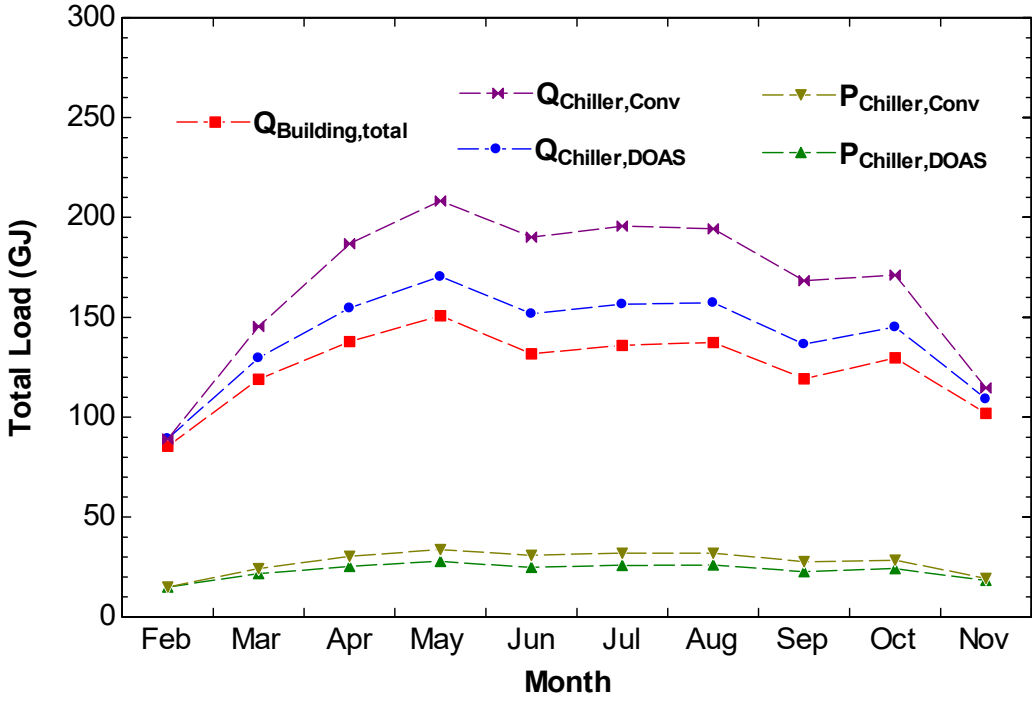

Figure 9. Variation of monthly building total load, chiller cooling load, and chiller energy consumption with and without the DOAU system for Kolkata.

Weather data analysis for Kolkata shows that outdoor temperature is highest for May, and the humidity ratio is highest for July. Also, building cooling demand is highest in May due to high ambient temperature and solar heat gains.

Figure 10 shows the hourly variation of the conditioned space temperature (Ground, first, second, and third floor) and ambient temperature for the first week of May for Kolkata. As per the schedule, the chiller plant starts at 7 A.M (Table 2) when there are no students inside the class, which results in a sharp zone temperature drop at the start. The zone temperatures again increase at about 8 A.M when the class starts. The PID controller maintains the zones at a set temperature for desired thermal comfort. The graph shows a sharp change in temperature profile due to the lunch break from 1 to 2 PM when no students are present in the classroom. As no class is scheduled for the weekend (Saturday and Sunday), a rise in zone temperature during weekends can be observed from the figure.

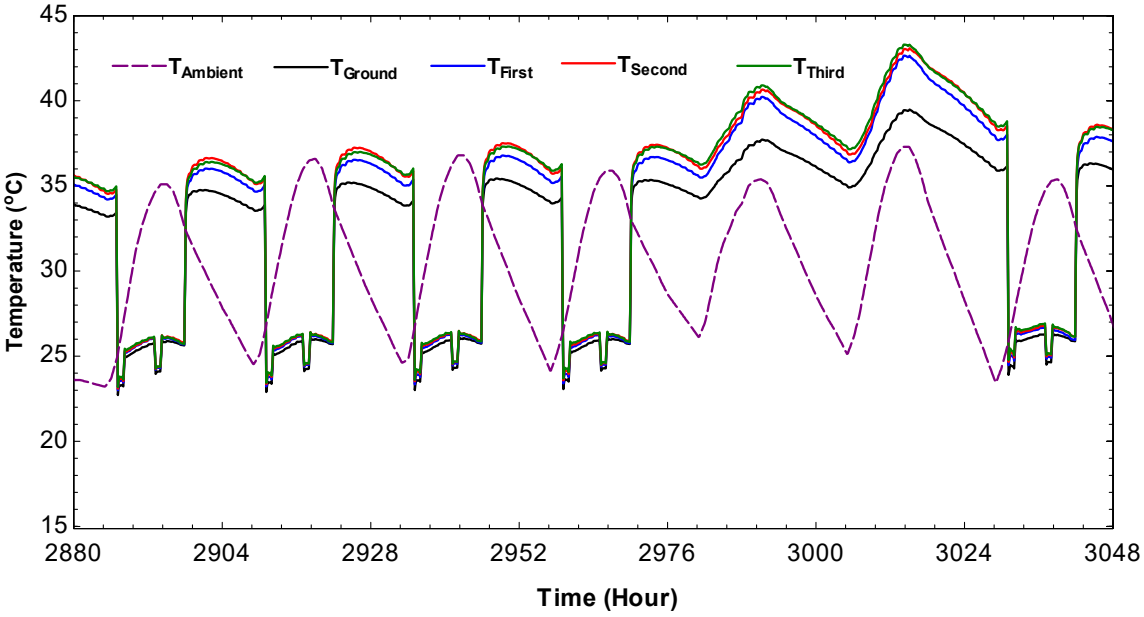

Figure 10. Hourly variation of ambient and building zone temperatures for the first week of May for Kolkata.

Figure 11 shows the hourly variation of conditioned space relative humidity (Ground, first, second, and third floor) and ambient relative humidity for the first week of July for Kolkata. From the figure, it is clear that zone relative humidity is maintained within the desirable limits during the class schedule to maintain the thermal comfort of the occupants. A sharp change in humidity is observed during the starting and end of class as the system undergoes a transient to steady state phase or vice versa. The graph shows a drop in humidity level during lunch break as no students are present inside the classroom during the break.

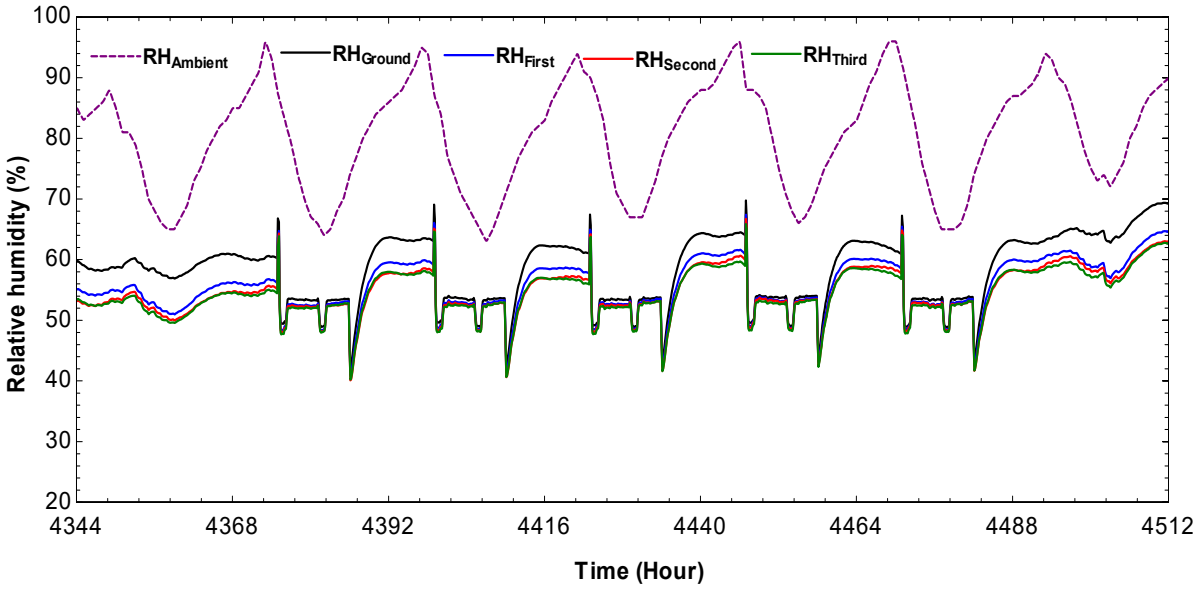

Figure 11. Hourly variation of ambient and building zone relative humidity for the first week of July for Kolkata.

Figure 12 shows the hourly variation of building total load, building sensible load and total cooling coil capacity (coil 1 and 2) for the first week of May for Kolkata. From the graph, it is seen that the contribution of building latent cooling demand is significant due to a large occupancy. The total cooling coil capacity is higher than building total load to maintain ventilation standards due to high occupancy. The sharp increase in cooling demand at 8 A.M is due to the sudden entry of students inside the classroom, which rapidly changes internal cooling demand. The change in building cooling demand due to the lunch break from 1 to 2 P.M can also be observed from the figure.

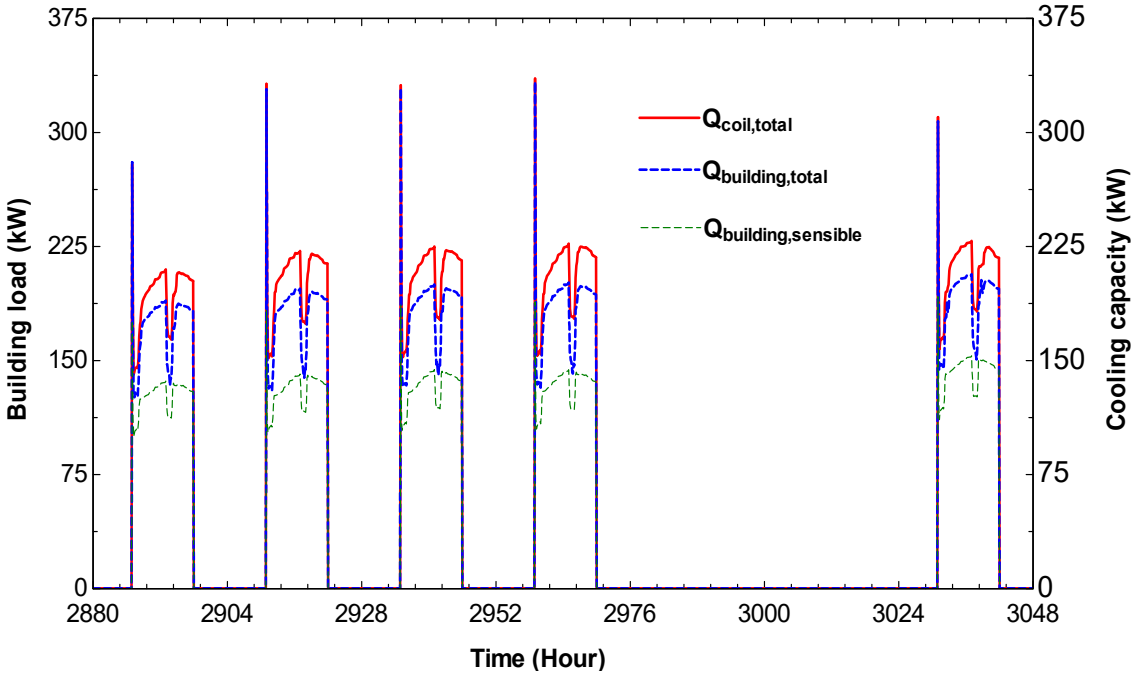

Figure 12. Hourly variation of building total load, building sensible load, and total cooling coil capacity for the first week of May for Kolkata.

Figure 13 shows the hourly variation of the total and sensible capacity of coil-1 and coil-2 for the first week of May for Kolkata when cooling demand is very high. The graph shows that the cooling capacity of coil-1 and coil-2 changed as per the classroom schedule. A sharp increase in cooling demand is observed in class starting with sudden student entry, which again changes during lunch break from 1 to 2 PM. Coil-1 handle more latent load than coil-1. As shown in the figure, Coil-2 handles the maximum amount of sensible load with a small amount of latent load as it is placed after the DOAU, i.e., enthalpy and desiccant wheels.

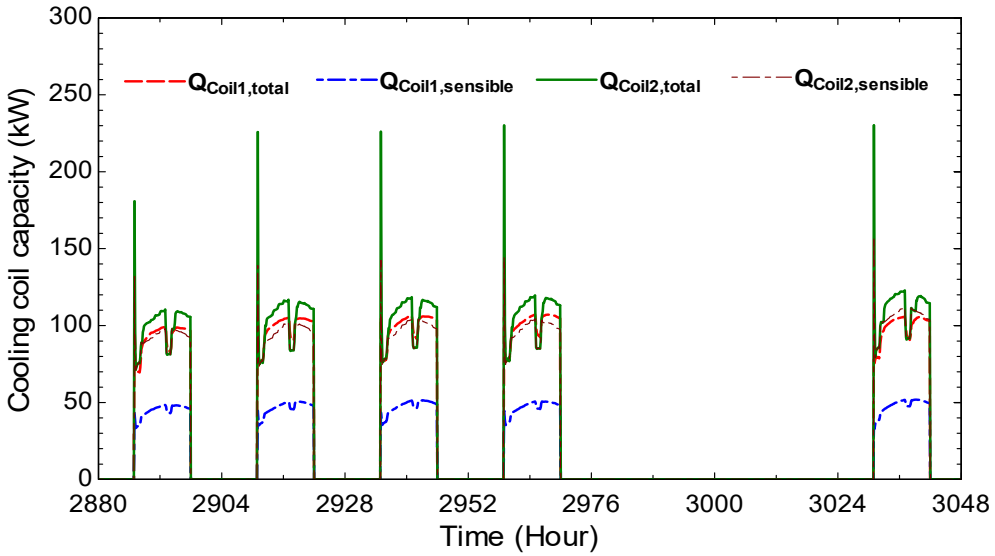

Figure 13. Hourly variation of cooling coil-1 and coil-2 total and sensible cooling capacity for the first week of May for Kolkata.

The chilled water required for cooling and dehumidifying the air is supplied to Cooling Coils 1 and 2 by a water-cooled chiller (Type 666). Figure 14 illustrates the hourly variation of chiller cooling load, load met by the chiller, chiller power consumption, and coefficient of performance (COP) for the first week of May with DOAU for Kolkata. The chiller cooling load ($Q_{chiller}$) represents the cooling demand imposed by the cooling coils at a given simulation time step to maintain the desired indoor thermal comfort conditions. The met cooling load (Q_{met}) denotes the actual cooling delivered by the chiller. It is observed from the figure that $Q_{chiller}$ and Q_{met} follow the same trend and remain equal throughout the period, indicating that the chiller is adequately sized and capable of meeting the required cooling demand at all time instants. A sharp increase in both chiller cooling load and power consumption is observed at the beginning of operation, which can be attributed to sudden changes in air and chilled water inlet conditions as the system transitions from ambient conditions to the prescribed set points. Furthermore, variations in chiller load and power during the day correspond to occupancy patterns, with increased loads during class hours due to student occupancy and reduced loads during lunch breaks when no classes are scheduled.

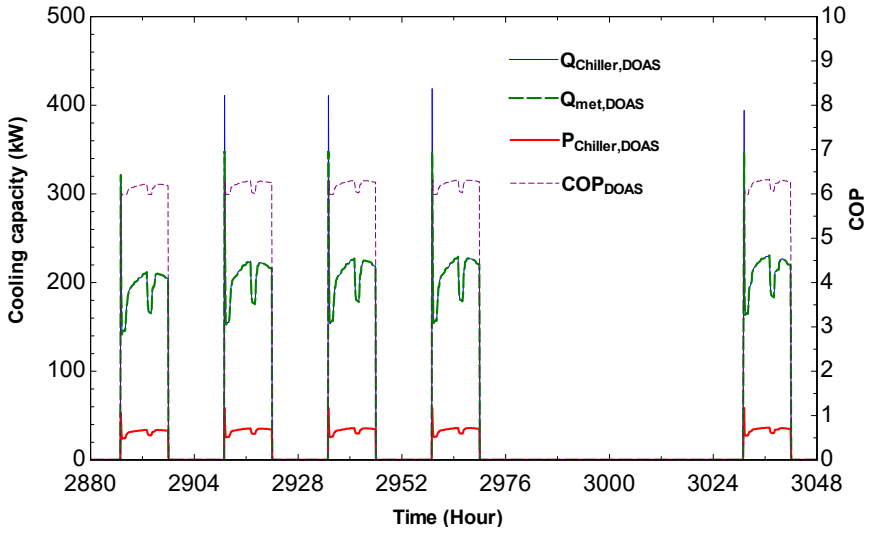

Figure 14. Hourly variation of chiller cooling load, chiller load met, chiller input power, and COP with DOAU system for first week of May for Kolkata.

Figure 15 shows the hourly variation of process and regeneration air temperature at exit of enthalpy and desiccant wheel for first week of May for Kolkata. The enthalpy wheel transfers heat between process and regeneration air streams due to temperature difference. The graph shows that the temperature of regeneration air at the exit of enthalpy wheel is more than temperature of exit process air at any time instant. Similarly, the temperature of process air at exit of desiccant wheel is less than that of exit regeneration air at any time instant.

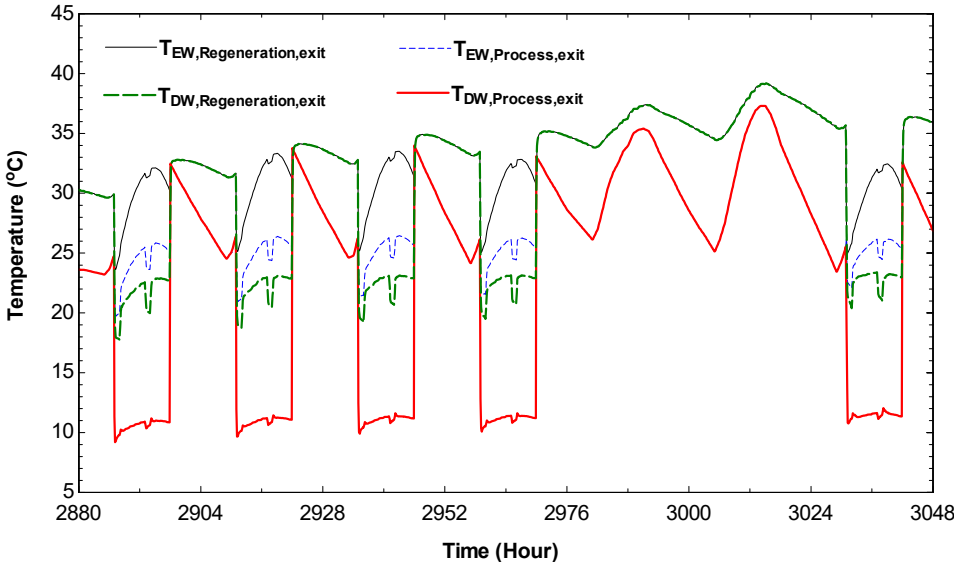

Figure 15. Hourly variation of process and regeneration air temperature at the exit of the enthalpy and desiccant wheel for the first week of May for Kolkata.

The regeneration air temperature at the exit of desiccant wheel is same as regeneration air temperature at inlet of enthalpy wheel, which is in between the exit process air temperature of desiccant wheel and exit regeneration air temperature of enthalpy wheel as shown in graph. Figure shows that temperatures follow the schedule of the classroom working hours.

Figure 16 shows the percentage savings in chiller cooling load and energy consumption of the centrally conditioned educational building complex with the DOAU system from February to November for Kolkata. Results show that the % reduction in chiller cooling load and energy consumption are more for monsoon months compared to summer months.

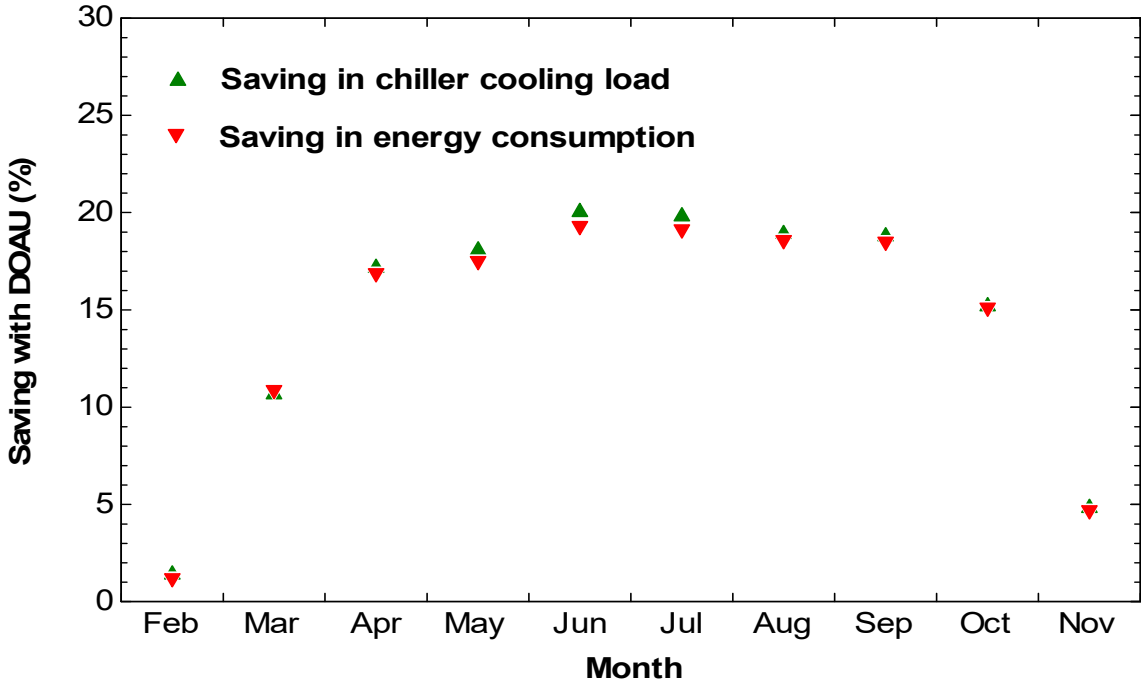

Figure 16. Percentage (%) saving in chiller cooling load and energy consumption with DOAU for Kolkata**.**

Table 7 shows the summary of annual chiller cooling load and annual energy consumption with and without the DOAU system for Kolkata and Jodhpur. Results show that with the implementation of DOAU, the annual reductions in chiller load and energy consumption are 18.0% and 17.5% for Kolkata, and 6.2% and 5.9% for Jodhpur, respectively. The purpose of comparing the results of a hot-humid climate with a hot-dry climate is to assess the suitability of the DOAU system for different climatic conditions in India. Based on the results, it may be concluded that the DOAU system is more effective in hot-humid climates than in hot-dry climates, as the system is capable to handle a higher latent load due to the higher humidity in hot-humid climates.

Table 7. Summary of annual chiller cooling load, energy consumption and % saving with DOAU system for Kolkata (hot and humid), Jodhpur (hot and dry), from February to November.

Parameters	Kolkata			Jodhpur		
	with DOAU	without DOAU	% Saving with DOAU	with DOAU	without DOAU	% Saving with DOAU
Annual cooling load (GJ)	1400.2	1709.3	18.0	1205.2	1285.1	6.2
Annual energy consumption (GJ)	230.9	279.9	17.5	199.5	212.1	5.9

The enthalpy wheel associated with the DOAU system plays a very vital role in reduction of required cooling coil capacity by decreasing temperature and humidity ratio of supply air while interacting with outgoing exhaust air of conditioned classroom. Furthermore, it is very important to mention that DOAU is not only expensive but also subject to performance (effectiveness) degradation over time, needing periodic replacement of the wheel. So, it is interesting to know the exact depreciation rate and its effect on the cooling coil capacity. There are three possibilities of degradation of wheel performance:

- Case-1: Enthalpy wheel sensible and latent effectiveness degrade at the same rate, which is more realistic situation associated with the DOAU system
- Case-2: Enthalpy wheel sensible effectiveness is constant while latent effectiveness degrades with time
- Case-3: Enthalpy wheel latent effectiveness is constant while sensible effectiveness degrades with time

Figure 17 shows the variation of enthalpy wheel sensible and latent effectiveness (case-1) with total cooling coil capacity, coil-1 and coil-2 cooling capacity for Kolkata. From the results, it is concluded that total cooling coil capacity increases with a decrease in the effectiveness of the wheel. The effect of wheel degradation is more for coil-1 because it is placed just after the enthalpy wheel, compared to coil-2, which is associated with the AHU. Figure 18 shows the variation of coil-1 and coil-2 sensible and latent cooling capacity with wheel sensible and latent effectiveness for Kolkata. From the graph, it is clear that effect of decrease in wheel effectiveness is more dominating for latent cooling capacity of coil-1 and 2. The effect of wheel degradation is almost negligible for the sensible cooling capacity of coil-2.

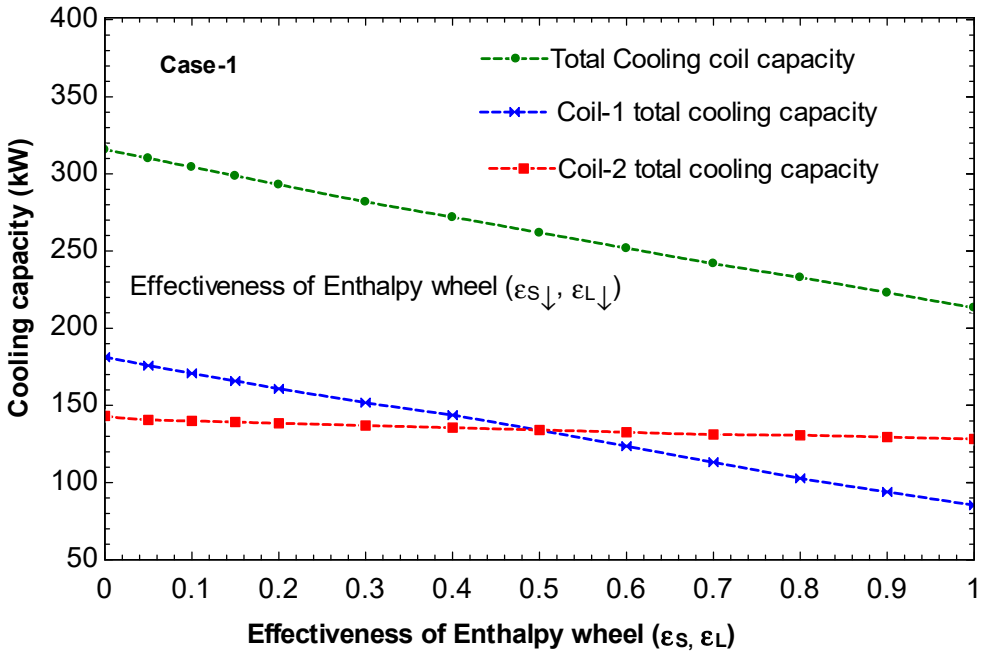

Figure 17. Variation of cooling coil capacity with the effectiveness of the enthalpy wheel for Kolkata.

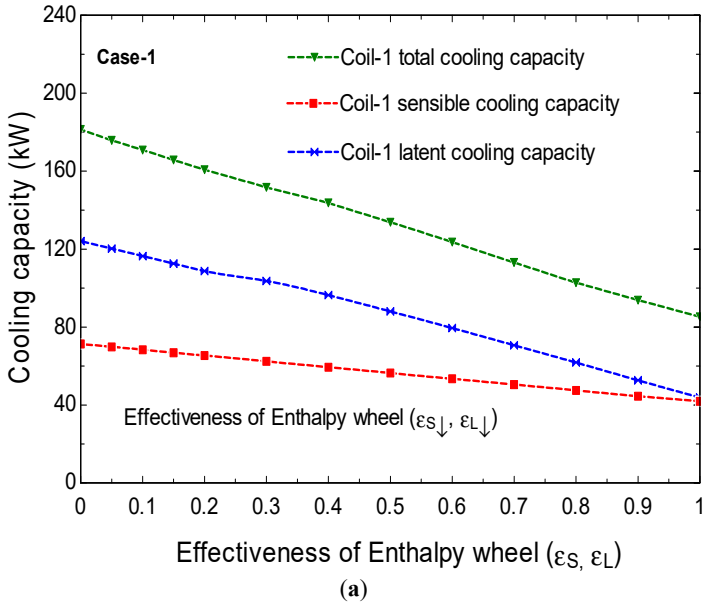

(a)

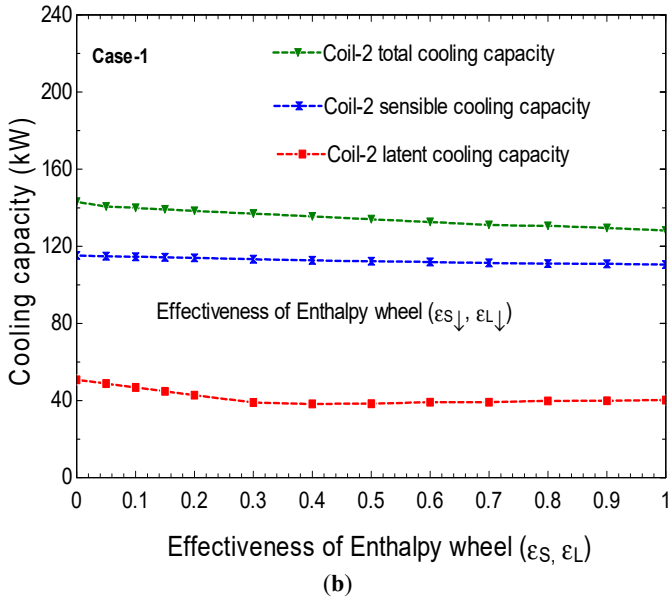

Figure 18. Variation of coil-1 (**a**) and coil-2 (**b**) cooling capacity with the effectiveness of the enthalpy wheel for Kolkata.

The sensible effectiveness of the enthalpy wheel basically depends upon the geometry of the wheel, flow rate and the temperature difference of air streams. The variation in sensible effectiveness of enthalpy wheel can controlled with proper and scheduled maintenance of wheel and air filters. Figure 19 shows the variation of cooling coil capacity with variation of latent effectiveness while sensible effectiveness (ε_S = 0.67) of enthalpy wheel is constant (case-2). From the graph, it is clear that total cooling coil capacity, coil-1 and coil-2 cooling capacity increase with decrease in latent effectiveness of enthalpy wheel. The effect of latent effectiveness on wheel degradation is more dominating for coil 1 compared to coil 2.

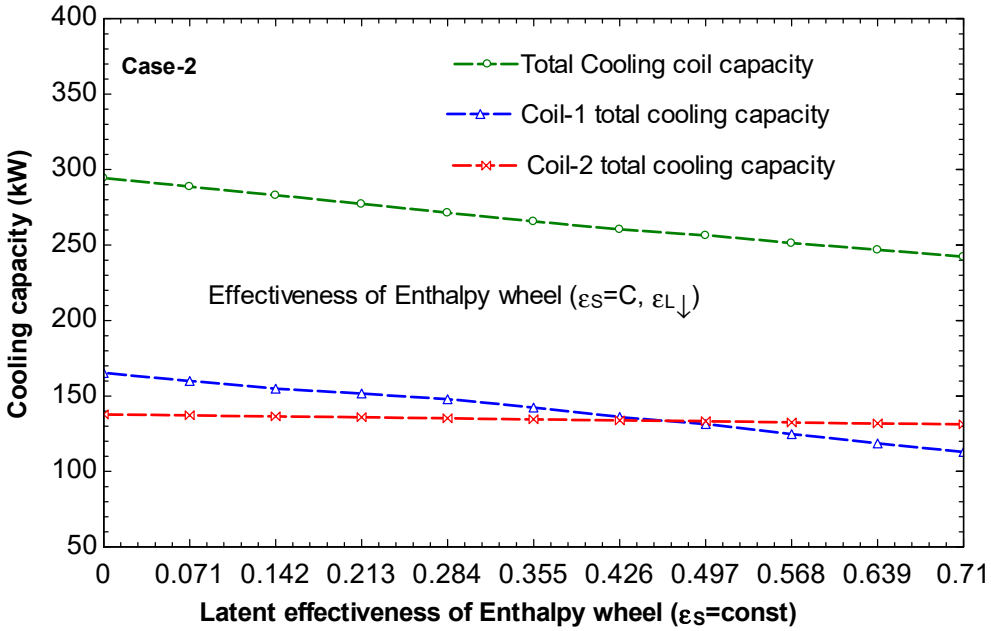

Figure 19. Variation of cooling coil capacity with variation of latent effectiveness (ε_S = C) of enthalpy wheel for Kolkata.

Figure 20 shows the variation of cooling coil capacity with variation of sensible effectiveness, while latent effectiveness (ε_L = 0.71) of enthalpy wheel is constant (case-3) for Kolkata. The results show that effect of sensible effectiveness degradation is very less on cooling coil capacity.

Finally, it can be concluded from the results that case 3 is more favourable for maintaining thermal comfort of a conditioned classroom with DOAU and AHU for hot-humid climates. However, in real life, it is challenging to maintain the constant latent effectiveness of an enthalpy wheel, as the latent effectiveness of the enthalpy wheel primarily depends on the hygroscopic desiccant material coated on the wheel, which degrades over time due to the continuous adsorption and desorption processes of air streams.

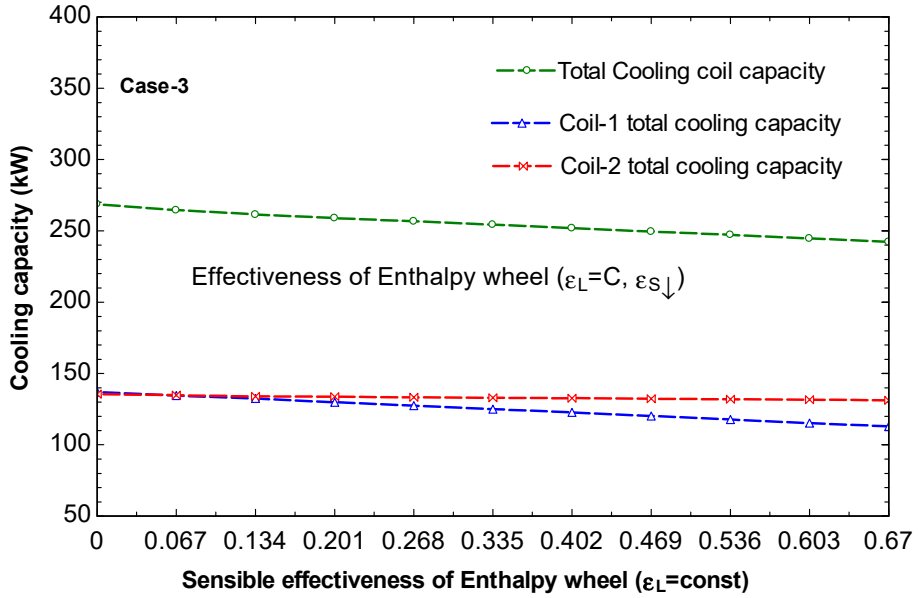

Figure 20. Variation of cooling coil capacity with variation of sensible effectiveness (ε_L = C) of enthalpy wheel for Kolkata.

The economic analysis of the conditioned classroom complex with the DOAU system is conducted for Kolkata and Jodhpur to assess the system's economic viability under different climatic conditions in India. The calculated Life cycle cost (LCC) with and without DOAU system for Kolkata is USD 216,400.0 and USD 219,200.0, and for Jodhpur is USD 205,978.6 and USD 198,960.4, considering a discount rate of 8%, electricity tariff (INR 8.94/kWh = USD 0.10/kWh), 25 years of lifespan of chiller and about 2,160 working hours over the year. The calculated simple payback period (PBP) for Kolkata is 4.9, and for Jodhpur is not feasible.

The electric tariff has a significant effect on the running cost of the chiller plant. Figure 21 illustrates the variation of LCC and PBP with changes in the electric tariff for Kolkata. The results indicate that the LCC with and without the DOAU system increases linearly with increasing electricity tariffs, whereas the payback period decreases nonlinearly.

The installation of the DOAU system is more favourable in regions with high electricity tariffs. The reduced energy cost improves economic performance, decreases the payback period, and lowers the LCC compared to conventional air conditioning.

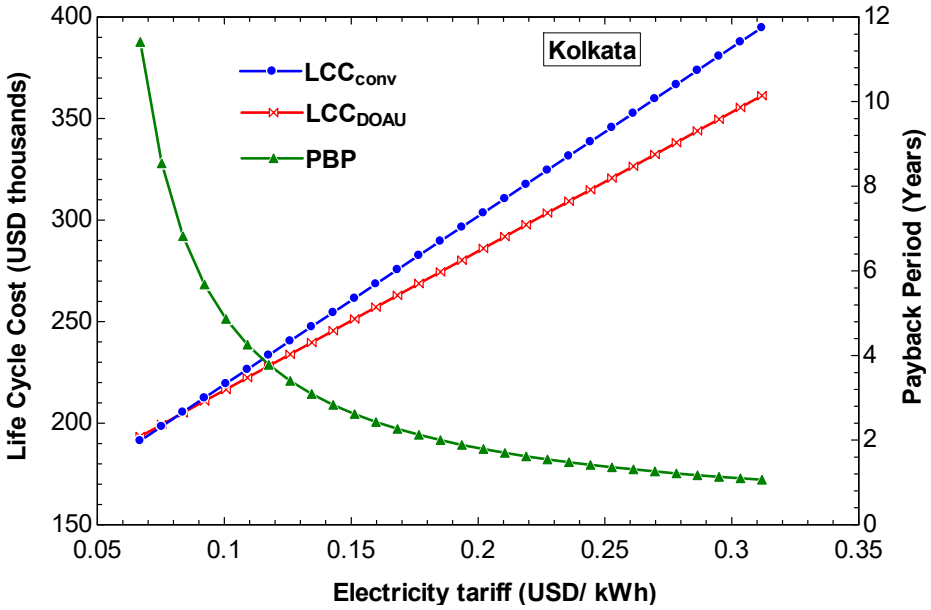

Figure 21. Variation of life cycle cost (LCC) and payback period (PBP) with electricity tariff for Kolkata.

Figure 22 illustrates the variation of LCC and PBP with changes in the electric tariff for Jodhpur. The results show that installation of the DOAU with conventional air conditioning is not economically viable for Jodhpur's climate due to higher LCC and a longer payback period when operated under the same electric tariff as Kolkata.

However, if the electric tariff exceeds a threshold limit, as shown by the vertical black line in Figure 22, this system may also become effective for hot-dry climates.

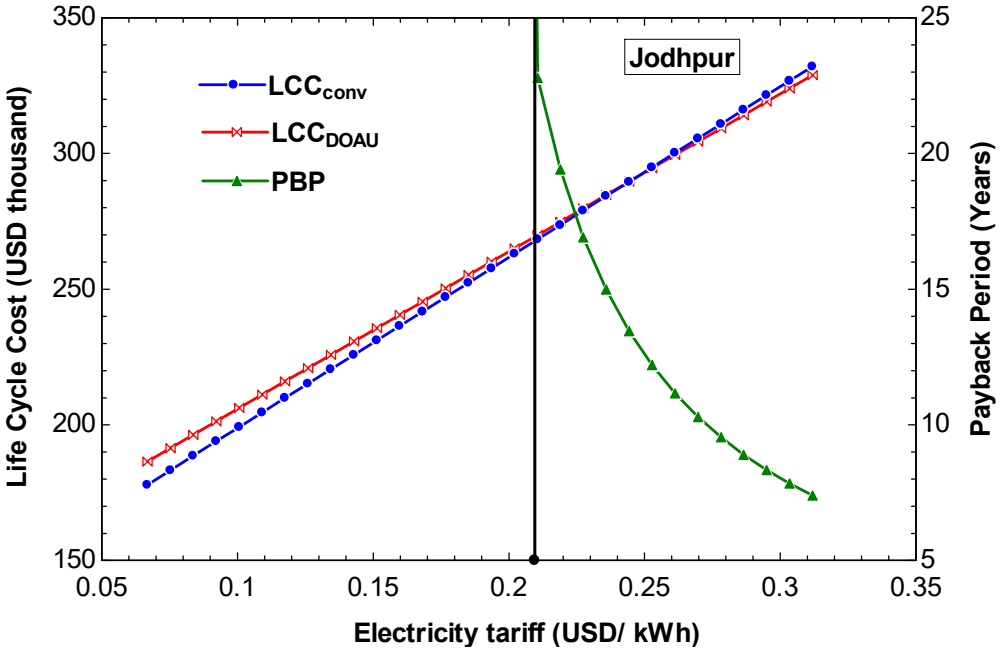

Figure 22. Variation of life cycle cost (LCC) and payback period (PBP) with electricity tariff for Jodhpur.

From the above analysis, it can be concluded that the DOAU system is not economically feasible for Jodhpur with the same inputs as Kolkata, as it results in a high LCC and a longer Payback period. However, as the DOAU system also offers environmental benefits in terms of lower carbon footprint, this conclusion may change if the environmental benefits take precedence over the economic benefits.

5. Conclusions

The performance of a centrally conditioned educational building complex located in Kharagpur (22.33° N, 87.32° E), close to Kolkata (22.57° N, 88.36° E), West Bengal, India, is evaluated. To assess the suitability of DOAU-based air conditioning for different climatic zones in India, the results are also compared with hot-dry climates, represented by Jodhpur (26.24° N, 73.02° E), Rajasthan, India.

The detailed analysis of the centrally conditioned educational building complex with DOAU and AHU is carried out using the TRNSYS model from February to November, as per chiller and classroom schedules. The enthalpy wheel and passive desiccant wheel of the DOAU system are regenerated by using low-temperature conditioned space air (26 °C) to eliminate the requirement of reheat coils. Using the TRNSYS model of the system, monthly building load, cooling coil capacity, chiller cooling load and energy consumption are estimated.

The building loads of the conditioned classroom complex for Kolkata and Jodhpur are compared. The results show that the building's total cooling load are almost the same for both climates during the monsoon months. However, latent load is more for Kolkata due to the humid outdoor conditions.

The annual chiller cooling load and energy consumption for Kolkata from February to November are 1400.2 GJ and 230.9 GJ with DOAU, and 1709.3 GJ and 279.9 GJ without DOAU, respectively. The percentage (%) reductions in annual chiller cooling load and energy consumption are around 18.0% and 17.5%, respectively.

The results for Jodhpur show that the annual chiller cooling load and energy consumption from February to November are 1205.2 GJ and 199.5 GJ with DOAU, and 1285.1 GJ and 212.1 GJ without DOAU, respectively. The percentage (%) reductions in annual chiller cooling load and energy consumption are around 6.2% and 5.9%, respectively. Overall, in terms of energy benefits, the DOAU system integrated with conventional air conditioning performs better in hot-humid climates.

The system evaluation is further analysed for a hot-humid climate, and results show that degradation of the enthalpy wheel of the DOAU system increases the required cooling coil capacity and power consumption to maintain the required thermal comfort of the classroom and may eventually lead to the replacement of these wheels for fixed chiller capacity. The effect of wheel depreciation rate is more dominating for cooling capacity of coil-1 compared to coil-2. The enthalpy wheel with constant latent effectiveness shows the most favourable condition for the implementation in a centrally conditioned classroom with DOAU and AHU.

To assess the economic viability of the DOAU system for Kolkata and Jodhpur, the results are compared based on the calculated LCC and payback period. However, the results show that the system is suitable for Jodhpur, which has a hot-dry climate, only if the electric tariff exceeds the threshold.

The results of the economic analysis for Kolkata show that a cooling system with DOAU has a lower LCC value compared to a conventional system. The calculated simple payback period with DOAU, considering constant effectiveness of the enthalpy wheel (ε_S = 0.67, ε_L = 0.71) and electric tariff (USD 0.10/kWh), is 4.9 years. Higher electric tariffs favour the use of the DOAU system for other climatic conditions in India.

Based on the above results, it may be concluded that the use of the DOAU system offers an energy-efficient solution for high occupancy buildings located in hot and humid climatic conditions.

The present work is expected to provide a systematic framework for evaluating the use of the DOAU system. Since reduction in energy consumption with DOAU leads to environmental benefits, a detailed techno-economic-environmental analysis is needed to establish the full benefits of the energy recovery DOAU in real buildings.

Author Contributions

D.B.: conceptualization, methodology, software, data curation, investigation, visualization, writing—original draft preparation; M.G.: supervision, investigation, visualization, writing—reviewing and editing. All authors have read and agreed to the published version of the manuscript.

Funding

This research received no external funding.

Institutional Review Board Statement

Not applicable.

Informed Consent Statement

Not applicable.

Data Availability Statement

All data used is presented in the paper.

Acknowledgements

The authors acknowledge the School of Energy Science and Engineering, Indian Institute of Technology Kharagpur, West Bengal-721302, for providing access to the TRNSYS software and other resources to carry out the research.

Conflicts of Interest

The authors declare no conflict of interest.

Use of AI and AI-Assisted Technologies

During the preparation of the manuscript, the authors used Grammarly (Grammarly Inc.) for English correction, proofreading and editing. After using this tool, the authors reviewed and edited the content as needed and take full responsibility for the content of the published article.

Nomenclature

c_p	Specific heat at constant pressure (kJ/kg-K)
C_E	Annual energy cost (USD)
C_0	Total initial cost (USD)
C_{MR}	Annual maintenance and repair cost (USD)
C_R	Replacement cost (USD)
d	Discount rate (%)
h_{fg}	Heat of vaporization of water (kJ/kg)
$\dot{m}$	Mass flow rate (kg/s)
n	Life span (Year)
$P_{chiller}$	Chiller input power
Q_{avil}	Available cooling capacity of chiller at current time step (kW)

$Q_{C,S}$	Sensible cooling coil capacity (kW)
$Q_{C,L}$	Latent cooling coil capacity (kW)
$Q_{C,t}$	Total cooling coil capacity (kW)
Q_{Conv}	Cooling coil capacity with conventional system (kW)
$Q_{chiller}$	Chiller cooling load demand at current time step (kW)
Q_{met}	Cooling load that chiller is capable to meet at current time step (kW)
Q_{rated}	Chiller rated capacity (kW)
R_c	Chiller capacity ratio
S_n	Salvage value cost at the end of life (kW)
T_d	Dry bulb temperature (°C)
AHU	Air handling unit
ASHRAE	American Society of Heating, Refrigerating, and Air Conditioning Engineers
CFD	Computational fluid dynamics
COP	Coefficient of performance
DBT	Dry bulb temperature (°C)
DOAU	Dedicated outdoor air unit
ERV	Energy recovery ventilator
F_{PL}	Fraction of Full Load Power
HVAC	Heating ventilation and air conditioning
INR	Indian Rupee (₹)
LCC	Life Cycle Cost (USD)
PBP	Payback period (Years)
PLR	Part Load Ratio
RH	Relative humidity (%)
SBS	Sick building syndrome
USD	United States dollar ($)
VAV	Variable air volume
Subscripts	
1,2,3…etc.	Reference state points
Conv, DW, EW	Conventional, Desiccant wheel, Enthalpy wheel
L, S, t	Latent, sensible, total
Greek symbols	
ω	Specific humidity (kg /kg air)
ε_L	Latent effectiveness of enthalpy wheel
ε_S	Sensible effectiveness of enthalpy wheel

References

1. Pal, R.; Roy, S.; Thakur, B. Assessment of Energy Efficiency for Traditional Non-Engineered and Engineered Residential Buildings—A Case of North-Eastern India. *Mater. Today Proc.* **2022**, *61*, 440–451. https://doi.org/10.1016/j.matpr.2021.11.538.
2. Kaushal, A.A.; Anand, P.; Aithal, B.H.; et al. Thermal Comfort in Indian Naturally Ventilated Buildings: A Comprehensive Review. *Energy Build.* **2024**, *306*, 113923. https://doi.org/10.1016/j.enbuild.2024.113923.
3. Lombard, L.P.; Ortiz, J.; Pout, C. A Review on Buildings Energy Consumption Information. *Energy Build.* **2008**, *40*, 394–398. https://doi.org/10.1016/j.enbuild.2007.03.007.
4. EPA. Available online: https://www.epa.gov/coronavirus/ventilation-and-coronavirus-covid-19 (accessed on 7 July 2024).
5. Jani, D.B.; Mishra, M.; Sahoo, P.K. Exergy Analysis of Solid Desiccant-Vapor Compression Hybrid Air Conditioning System. In Proceedings of the 23rd National Heat and Mass Transfer Conference and 1st International ISHMT-ASTFE Heat and Mass Transfer Conference, Thiruvananthapuram, India, 17–20 December 2015.
6. Burns, P.R.; Mitchell, J.W.; Beckman, W.A. Hybrid Desiccant Cooling Systems in Supermarket Applications. *ASHRAE Trans.* **1985**, *91*, 457–468.
7. Sheridan, J.C.; Mitchell, J.W. A Hybrid Solar Desiccant Cooling System. *Sol. Energy* **1985**, *34*, 187–193. https://doi.org/10.1016/0038-092X(85)90179-3.
8. Jain, S.; Dhar, P.L.; Kaushik, S.C. Evaluation of Solid Based Evaporative Cooling Cycles for Typical Hot and Humid Climates. *Int. J. Refrig.* **1995**, *18*, 287–296. https://doi.org/10.1016/0140-7007(95)00016-5.
9. Mumma, S.A.; Shank, K.M. Achieving Dry Outside Air in an Energy-Efficient Manner. *ASHRAE Trans.* **2001**, *107*, 553–561.
10. Dhar, P.L.; Singh, S.K. Studies on Solid Desiccant Based Hybrid Air-Conditioning. *Appl. Therm. Eng.* **2001**, *21*, 119–134. https://doi.org/10.1016/S1359-4311(00)00035-1.
11. Zhang, L.Z.; Niu, J.L. Energy Requirements for Conditioning Fresh Air and the Long-Term Savings with a Membrane-Based Energy Recovery Ventilator in Hong Kong. *Energy* **2001**, *26*, 119–135. https://doi.org/10.1016/S0360-5442(00)00064-5.
12. Subramanyam, N.; Maiya, M.; Murthy, S. Application of Desiccant Wheel to Control Humidity in Air-Conditioning Systems. *Appl. Therm. Eng.* **2004**, *24*, 2777–2788. https://doi.org/10.1016/j.applthermaleng.2004.04.008.
13. Zhou, Y.; Wu, J.; Wang, R. Performance of Energy Recovery Ventilator with Various Weathers and Temperature Set-Points. *Energy Build.* **2007**, *39*, 1202–1210. https://doi.org/10.1016/j.enbuild.2006.12.010.

14. Hao, X.; Zhang, G.; Chen, Y.; et al. A Combined System of Chilled Ceiling, Displacement Ventilation and Desiccant Dehumidification. *Build. Environ.* **2007**, *42*, 3298–3308. https://doi.org/10.1016/j.buildenv.2006.08.020.
15. Chen, Q. Ventilation Performance Prediction for Buildings: A Method Overview and Recent Applications. *Build. Environ.* **2009**, *44*, 848–858. https://doi.org/10.1016/j.buildenv.2008.05.025.
16. Baniyounes, A.M.; Liu, G.; Rasul, M.G.; et al. Analysis of Solar Desiccant Cooling System for an Institutional Building in Subtropical Queensland, Australia. *Renew. Sustain. Energy Rev.* **2012**, *16*, 6423–6431. https://doi.org/10.1016/j.rser.2012.07.021.
17. Guidara, Z.; Elleuch, M.; Bacha, H.B. New Solid Desiccant Solar Air Conditioning Unit in Tunisia: Design and Simulation Study. *Appl. Therm. Eng.* **2013**, *58*, 656–663. https://doi.org/10.1016/j.applthermaleng.2013.05.005.
18. Murray, P.; Rysanek, A.M.; Pantelic, J.; et al. On Decentralized Air-Conditioning for Hot and Humid Climates: Performance Characterization of a Small Capacity Dedicated Outdoor Air System with Built-in Sensible and Latent Energy Recovery Wheels. *Energy Procedia* **2015**, *78*, 3471–3476. https://doi.org/10.1016/j.egypro.2015.12.332.
19. Jani, D.B.; Mishra, M.; Sahoo, P.K. Experimental Investigation on Solid Desiccant Vapor Compression Hybrid Air Conditioning System in Hot and Humid Weather. *Appl. Therm. Eng.* **2016**, *104*, 556–564. https://doi.org/10.1016/j.applthermaleng.2016.05.104.
20. O'Connor, D.; Calautit, J.K.; Hughes, B.R. A Novel Design of a Desiccant Rotary Wheel for Passive Ventilation Applications. *Appl. Energy* **2016**, *179*, 99–109. https://doi.org/10.1016/j.apenergy.2016.06.029.
21. Jani, D.B.; Mishra, M.; Sahoo, P.K. Performance Analysis of a Solid Desiccant Assisted Hybrid Space Cooling System Using TRNSYS. *J. Build. Eng.* **2018**, *19*, 26–35. https://doi.org/10.1016/j.jobe.2018.04.016.
22. Chen, L.; Chen, S.H.; Liu, L.; et al. Experimental Investigation of Precooling Desiccant-Wheel Air-Conditioning System in a High-Temperature and High-Humidity Environment. *Int. J. Refrig.* **2018**, *95*, 83–92. https://doi.org/10.1016/j.ijrefrig.2018.08.015.
23. Herath, H.M.D.P.; Wickramasinghe, M.D.A.; Polgolla, A.M.C.K.; et al. Applicability of Rotary Thermal Wheels to Hot and Humid Climates. *Energy Rep.* **2020**, *6*, 539–544. https://doi.org/10.1016/j.egyr.2019.11.116.
24. Su, M.; Han, X.; Chong, D.; et al. Experimental Study on the Performance of an Improved Dehumidification System Integrated with Precooling and Recirculated Regenerative Rotary Desiccant Wheel. *Appl. Therm. Eng.* **2021**, *199*, 117608. https://doi.org/10.1016/j.applthermaleng.2021.117608.
25. Bhabhor, K.K.; Jani, D.B. Performance Analysis of Desiccant Dehumidifier with Different Channel Geometry Using CFD. *J. Build. Eng.* **2021**, *44*, 103021. https://doi.org/10.1016/j.jobe.2021.103021.
26. Herath, H.M.D.P.; Wickramasinghe, M.D.A.; Polgolla, A.M.C.K.; et al. CFD-Based Analysis of Heat Exchanging Performance of Rotary Thermal Wheels. In *Sustainability in Energy and Buildings 2020*; Littlewood, J., Howlett, R.J., Jain, L.C., Eds.; Springer: Singapore, 2021; pp. 103–113. https://doi.org/10.1007/978-981-15-8783-2_8.
27. Tsai, H.Y.; Wu, C.T. Optimization of a Rotary Desiccant Wheel for Enthalpy Recovery of Air-Conditioning in a Humid Hospitality Environment. *Heliyon* **2022**, *8*, e10796. https://doi.org/10.1016/j.heliyon.2022.e10796.
28. Liu, M.; Tu, R.; Chen, X.H.; et al. Performance Analyses of an Advanced Heat Pump Driven Fresh Air Handling System Using Active and Passive Desiccant Wheels under Various Weather Conditions. *Int. J. Refrig.* **2022**, *141*, 1–11. https://doi.org/10.1016/j.ijrefrig.2022.04.017.
29. Wang, H.; Liu, L.; Liu, L.X.; et al. Performance Analysis of Different Air Conditioning Systems in Apartment Buildings under Different Climates in China. *Int. J. Refrig.* **2022**, *139*, 192–203. https://doi.org/10.1016/j.ijrefrig.2022.04.007.
30. Cho, W.; Heo, J.; Park, M.H.; et al. Energy Performance and Thermal Comfort of Integrated Energy Recovery Ventilator System with Air-Conditioner for Passive Buildings. *Energy Build.* **2023**, *295*, 113302. https://doi.org/10.1016/j.enbuild.2023.113302.
31. Maqbool, S.; Maddali, R. Effect of System Configuration on the Performance of a Hybrid Air Conditioning System Based on R-1234yf. *Appl. Therm. Eng.* **2024**, *236*, 121624. https://doi.org/10.1016/j.applthermaleng.2023.121624.
32. Bandhu, D.; Ramgopal, M. Performance Evaluation of a Centrally Conditioned Classroom Complex with Energy Recovery: Energy and Environmental Analysis. *Heat Transfer Eng.* **2025**, 1–14. https://doi.org/10.1080/01457632.2025.2546266.
33. EnergyPlus. Available online: https://energyplus.net/weatherlocation/asia_wmo_region_2/IND/IND_Kolkata.428090_ISHRAE (accessed on 12 May 2026).
34. ASHRAE. *ASHRAE Handbook-Fundamentals*; Chapter 33; ASHRAE: Atlanta, GA, USA, 2017.
35. TESS—Thermal Energy System Specialists, LLC. *TESSLibs 17: Component Libraries for the TRNSYS Simulation Environment*; Version 17; TESS: Madison, WI, USA, 2010. Available online: https://www.trnsys.com/tess-libraries/TESSLibs17_General_Descriptions.pdf (accessed on 5 December 2025)
36. Jurinak, J.J. Open Cycle Solid Desiccant Cooling—Component Models and System Simulations. Ph.D. Thesis, University of Wisconsin-Madison, Madison, WI, USA, 1982.
37. ASHRAE. ASHRAE Handbook-HVAC Systems and Equipment. In *Chapter 43: Liquid Chillers*; ASHRAE: Atlanta, GA, USA, 2024.

38. U.S. Department of Energy. *EnergyPlus Engineering Reference*; DOE: Washington, DC, USA, 2022.
39. Thermal Energy System Specialists (TESS). *TESSLibs 17, Vol. 06: HVAC Library Mathematical Reference*; TESS: Madison, WI, USA, 2012; pp. 214–218.
40. Bry-Air (Asia) Pvt. Ltd. *Desiccant Dehumidification Systems and Wheels: Technical Specifications and Maintenance Guidelines*; Bry-Air (Asia) Pvt. Ltd.: Gurugram, India, 2021. Available online: https://www.bryair.com/products/ (accessed on 5 December 2025).
41. HVAC: Air Treatment Engineering Pvt. Ltd. *HVAC System Design Manual for Nalanda Building*; Air Treatment Engineering Pvt. Ltd.: Chennai, India, 2014.
42. ASHRAE. Energy Recovery Devices. In *ASHRAE Handbook—HVAC Systems and Equipment*; ASHRAE: Atlanta, GA, USA, 2020. Available online: https://www.ashrae.org/file%20library/technical%20resources/covid-19/si_s20_ch26.pdf (accessed on 5 December 2025).
43. Desiccant Rotors International Pvt. Ltd. *Desiccant and Enthalpy Wheel Products: Technical Specifications*; Desiccant Rotors International Pvt. Ltd.: Gurugram, India, 2025. Available online: https://www.drirotors.com/product/energy-recovery-rotors-wheels/ (accessed on 5 December 2025).
44. Available online: https://hmc.iitkgp.ac.in/web/wp-content/uploads/2017/06/OO-Electricity-Tariff.pdf (accessed on 12 May 2026).
45. Tiwari, A.; Kushwaha, P.K.; Agrawal, A.; et al. Performance Evaluation of a Solar-Assisted Air Conditioning System Based on Desiccant Wheel. *Therm. Sci. Eng. Prog.* **2025**, *68*, 104302. https://doi.org/10.1016/j.tsep.2025.104302.
46. Fuller, S.K.; Stephen, R.P. *Life-Cycle Costing Manual for the Federal Energy Management Program*; U.S. Department of Energy: Washington, DC, USA, 1996.
47. *ISO 15686-1:2011*; Buildings and Constructed Assets—Service Life Planning—Part 1: General Principles/Frameworkbiao. International Organization of Standardization: Geneva, Switzerland, 2008.
48. Kirk, S.J.; Dellisola, A.J. *Life Cycle Costing for Design Professionals*, 2nd ed.; McGraw-Hill, Inc.: Columbus, OH, USA, 1995.
49. Murugavel, V.; Saravanan, R. Life Cycle Cost Analysis of Waste Heat Operated Absorption Cooling Systems for Building HVAC Applications. In Proceedings of the Tenth International Conference Enhanced Building Operations, Kuwait City, Kuwait, 26–28 October 2010.
50. Maqbool, S.; Bandhu, D.; Maddali, R. Performance of Hybrid Air Conditioning Systems with Split Condenser and Evaporator. *Sādhanā* **2025**, *50*, 262. https://doi.org/10.1007/s12046-025-02879-8.
51. Maqbool, S.; Ramgopal, M. Performance of a CO_2 Based Hybrid Air Conditioning System for Hot and Humid Climates. *Appl. Therm. Eng.* **2025**, *274*, 126602. https://doi.org/10.1016/j.applthermaleng.2025.126602.